Critical behavior of the random-field Ising model

Misha Gofman
School of Physics and Astronomy, Raymond and Beverly Sackler Faculty of Exact Sciences, Tel Aviv University, 69978, Tel Aviv, Israel

Joan Adler
School of Physics and Astronomy, Raymond and Beverly Sackler Faculty of Exact Sciences, Tel Aviv University, 69978, Tel Aviv, Israel and Department of Physics, Technion-IIT, 32000, Haifa, Israel

Amnon Aharony
School of Physics and Astronomy, Raymond and Beverly Sackler Faculty of Exact Sciences, Tel Aviv University, 69978, Tel Aviv, Israel

A. B. Harris
School of Physics and Astronomy, Raymond and Beverly Sackler Faculty of Exact Sciences, Tel Aviv University, 69978, Tel Aviv, Israel and Department of Physics, University of Pennsylvania, Philadelphia, Pennsylvania 19104

Moshe Schwartz
School of Physics and Astronomy, Raymond and Beverly Sackler Faculty of Exact Sciences, Tel Aviv University, 69978, Tel Aviv, Israel
(Received 19 July 1995)

We study the critical properties of the random field Ising model in general dimension d using high-temperature expansions for the susceptibility, $\chi=\Sigma_j[\langle\sigma_i\sigma_j\rangle_T-\langle\sigma_i\rangle_T\langle\sigma_j\rangle_T]_h$ and the structure factor, $G=\Sigma_j[\langle\sigma_i\sigma_j\rangle_T]_h$, where $\langle\rangle_T$ indicates a canonical average at temperature T for an arbitrary configuration of random fields and $[]_h$ indicates an average over random fields. We treated two distributions of random fields, the bimodal in which each $h_i=\pm h_0$ and a Gaussian distribution in which each h_i has variance h_0^2. We obtained series for χ and G in the form $\Sigma_{n=1,15}a_n(g,d)(J/T)^n$, where J is the exchange constant and the coefficients $a_n(g,d)$ are polynomials in $g\equiv h_0^2/J^2$ and in d. We assume that as T approaches its critical value, T_c, one has $\chi\sim(T-T_c)^{-\gamma}$ and $G\sim(T-T_c)^{-\bar{\gamma}}$. For dimensions above $d=2$ we find a range of values of g for which the critical exponents obtained from our series seem not to depend on g. For large values of g our results show a g dependence which is attributable to either a tricritical point or a first-order transition. All our results for critical exponents suggest that $\bar{\gamma}=2\gamma$, in agreement with the two-exponent scaling picture. In addition we have also constructed series for the amplitude ratio, $A=(G/\chi^2)(T^2)/(gJ^2)$. We find that A approaches a constant value as $T\rightarrow T_c$ (consistent with $\bar{\gamma}=2\gamma$) with $A\approx 1$. It appears that A is somewhat larger for the bimodal than for the Gaussian model, in agreement with a recent analysis at high d.

I. INTRODUCTION

In this paper we study the critical properties of the random field Ising model (RFIM). This model is defined by the Hamiltonian

$$\mathscr{H}=-J\sum_{\langle ij\rangle}\sigma_i\sigma_j-\sum_i h_i\sigma_i, \tag{1}$$

where $\langle ij\rangle$ indicates that the sum is over pairs of nearest neighboring sites and $\sigma_i=\pm 1$. We consider a hypercubic lattice in d spatial dimensions and the fields h_i are quenched random variables with no correlations between fields on different sites. Quenched thermodynamic averages are defined by

$$[\langle A\rangle_T]_h\equiv\left[\frac{\mathrm{Tr}(\exp(-\beta\mathscr{H})A)}{\mathrm{Tr}\,\exp(-\beta\mathscr{H})}\right]_h, \tag{2}$$

where $\beta=1/T$ ($k_B=1$) and $[]_h$ indicates an average over the distribution of the random fields at all sites. A similar definition gives the quenched free energy, F, as $F=[-T\ln Z]_h$, where $Z\equiv\mathrm{Tr}\,\exp(-\beta\mathscr{H})$ is the partition function associated with the Hamiltonian of Eq. (1). Here we consider two distributions for the h_i, namely the Gaussian, for which

$$P(h_i)=(2\pi h_0^2)^{-1/2}\exp[-h_i^2/(2h_0^2)] \tag{3}$$

and the bimodal, for which $h_i=\pm h_0$ with equal probability. We will express results in terms of the variables $g\equiv h_0^2/J^2$ and $K=\beta J$. As we shall discuss in more detail below, this system is interesting theoretically. Experimentally, it was not clear how one could obtain a random field whose spatial correlations were on the length scale of a lattice constant. However Fishman and Aharony[1] showed that a physical realization of the RFIM can be achieved by applying a uniform external field to a diluted Ising antiferromagnet (DIAF). Other experimental realizations of the RFIM are the diluted frustrated antiferromagnet[2] and binary liquids in porous media.[3–5]

The properties of the RFIM have been a subject of intense interest and much controversy both theoretically[6–30] and experimentally. We will not discuss the experimental results, since many of them, especially those from the early 1980's,

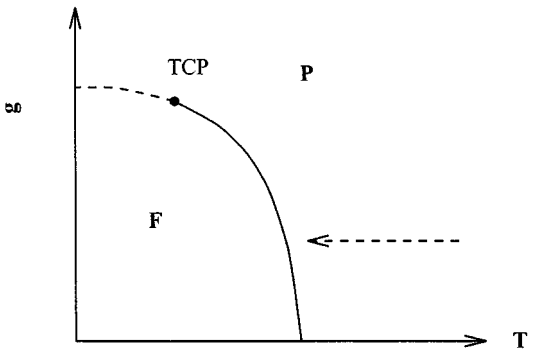

FIG. 1. Mean-field phase diagram for the random field Ising model. F (P) labels the ferromagnetic (paramagnetic) phase. For the bimodel distribution there is a tricritical point (TCP) below which temperature the transition becomes discontinuous, as indicated by the dashed line. For the Gaussian model there is no TCP at nonzero temperature. The dashed line parallel to the T axis indicates the way the critical line is approached by a high-temperature series.

are vitiated by the failure to achieve thermal equilibrium.[31–33] This phenomenon has been treated theoretically[34–36] and by simulations.[37–40] Here we review only those aspects of this model relevant to this paper. For a more general review of the RFIM, see Ref. 41. The most important problem is to clarify the behavior of this model in the limit of small but nonzero g. In a seminal work, Imry and Ma[6] argued that long-range ferromagnetic order was destroyed by the random field when d decreased below a critical value $d_<$ with $d_<=2$. They showed that the upper critical dimension, $d_>$, above which the critical behavior was mean-field like, was 6 and they gave results of the renormalization group ϵ expansion to first order in $\epsilon=6-d$. Shortly thereafter, systematic studies of the ϵ expansion[7–10] showed that it predicted that the critical exponents of the random system should be equal to those of the pure system but in a dimension lower by two ($d\to d-2$). This conclusion was earlier obtained exactly for the special case of the spherical model.[11] For a while it seemed that the problem had been solved by this idea of dimensional reduction. But difficulties with this picture became apparent. According to the Imry-Ma argument the lower critical dimension for the RFIM is two, whereas according to dimensional reduction ($d\to d-2$) it ought to be three. A careful confirmation of the Imry-Ma result ($d_<=2$) was given in Refs. 12, 13, and 14. More recently it has been proven rigorously by Imbrie[15,16] that the three-dimensional RFIM exhibits long-range order at $T=0$ and by Bricmont and Kupiainen[17,18] that the ordered phase does exist for a nonzero range of low temperatures for $d=3$. It is commonly believed that there is no long range order or any phase transition in two dimensions for $g>0$.

As we shall see, the qualitative features of the phase diagram in the T-g plane are of some relevance to our work. In an early study of the phase diagram, based on mean-field theory, Schneider and Pytte[42] considered a Gaussian distribution of random fields and found that the transition remained continuous along the whole phase boundary (see Fig. 1). As h_0^2 increases, they found that the transition temperature decreases until it becomes zero at $h_0/zJ=\sqrt{2/\pi}$, where z is the coordination number of the lattice. Aharony[43] also used mean-field theory to show that when the random field distribution has a relative minimum at zero field, the RFIM undergoes a first-order transition at sufficiently low temperature, and hence that there exists a tricritical point (see Fig. 1). For the bimodal distribution he found that the tricritical point occurs at $\beta zJ=3/2$, $\tanh^2(\beta h_0)=1/3$. Galam and Birman[44] later argued that even some distributions which had a local maximum at $h=0$ (but not the Gaussian) could give rise to a tricritical point. One would expect mean-field theory to be valid in high dimensions. However, the bimodal distribution on the Bethe lattice of coordination number $z=3$ was found *not* to have a tricritical point.[45] But later work of Galam and Salinas[46] showed that for $z>3$ the bimodal distribution on a Bethe lattice did have a tricritical point and that its location in the limit $z\to\infty$ was given by Aharony's result.[43] However, the existence of the tricritical point in finite dimensions need not follow the mean-field theory result.

The results of various numerical techniques (mostly for $d=3$) are not entirely clear. Young and Nauenberg[47] studied systems of size 64^3 spins with a bimodal distribution of random fields. Because their exponents violated some exact bounds they inferred a first order transition and suggested that the transition remained discontinuous even in the limit of small random fields. Ogielski and Huse[48] studying systems of size up to 32^3 found the transition to be continuous for the Gaussian model. They did not reach any firm conclusion for the bimodal distribution. Houghton *et al.*[49] tried to resolve this issue for general d by analyzing their seven-term high-temperature series expansion, whose coefficients were evaluated exactly in terms of the random field distribution, so that they could study T_c as a function of H_c. They interpreted that if H_c ceased to increase as T_c decreased, that behavior indicated the presence of a tricritical point. Their results based on this ansatz fitted nicely with the mean-field results: for the bimodal distribution they found a tricritical point in all $d\geqslant 3$. For the Gaussian distribution they found a tricritical point for $d=3$, whereas for d$\geqslant 4$ they claimed that there was no tricritical point, but their evidence does not seem definitive. More recently Rieger and Young[50] studied many realizations of systems of size 16^3 and for small values ($h_0=0.3$) of the random field (so as to make it easier to achieve equilibrium). From this work they concluded that the transition for the bimodal distribution was continuous for this value of h_0. There have also been suggestions that at sufficiently large random fields the system might have a spin-glass (SG) phase. Specifically, deAlmeida and Bruinsma (DAB) (Ref. 51) found such a phase at large d for a DIAF in a uniform field, which Fishman and Aharony[1] had shown to be in the same universality class as the RFIM. However, that equivalence does not exclude the possibility that the regime in which this happens could be different for the DIAF than for the RFIM. Working to second order in a parameter roughly equivalent to $T_c/(zT)$, where T_c is the transition temperature of the pure system, DAB found a multicritical point where antiferromagnetic (AF), SG, and paramagnetic phases coexist. A similar result was found numerically for $d=3$ in Ref. 40, for the dilute AF in a uniform field, H, but the fact that the SG phase appears even for $H=0$ casts some doubt on that work.

Next we review briefly the situation with regard to critical exponents in the regime where the transition is continuous.

Although there is controversy about the nature of the scaling at the critical point, there are some exact inequalities which the critical exponents must obey. These inequalities are phrased in terms of correlation functions at criticality for n-component spins. Strictly speaking these inequalities are obtained for a Gaussian distribution of random fields, but they are believed to apply to other distributions, such as the bimodal. One defines the following correlation functions and associated critical exponents. The structure factor behaves as

$$S(\mathbf{q}) \equiv [\langle \vec{\phi}_{\mathbf{q}} \cdot \vec{\phi}_{-\mathbf{q}} \rangle_T]_h \sim q^{-(4-\bar{\eta})}, \tag{4}$$

for $q \to 0$. Here $\vec{\phi}_{\mathbf{q}}$ is the spatial Fourier transform of the n-component spin variable which is the generalization of σ_i in the discrete model of Eq. (1). For small q, the $\mathbf{q}$-dependent susceptibility behaves as

$$\chi_{\mathbf{q}} \equiv [\langle \vec{\phi}_{\mathbf{q}} \cdot \vec{\phi}_{-\mathbf{q}} \rangle_T - \langle \vec{\phi}_{\mathbf{q}} \rangle_T \cdot \langle \vec{\phi}_{-\mathbf{q}} \rangle_T]_h \sim q^{-(2-\eta)}. \tag{5}$$

In this paper we will focus our attention on the susceptibility[52]

$$\chi(T,g) \equiv \sum_j [\langle \sigma_i \sigma_j \rangle_T - \langle \sigma_i \rangle_T \langle \sigma_j \rangle_T]_h = \chi(\mathbf{q}=0) \tag{6}$$

and the structure factor

$$G(T,g) \equiv \sum_j [\langle \sigma_i \sigma_j \rangle_T]_h = S(\mathbf{q}=0). \tag{7}$$

If one assumes a single correlation length ξ, then in the critical regime one has

$$\chi(T,g) \sim |T - T_c|^{-\gamma} \tag{8}$$

with $\gamma = (2-\eta)\nu$ and

$$G(T,g) \sim |T - T_c|^{-\bar{\gamma}} \tag{9}$$

with $\bar{\gamma} = (4-\bar{\eta})\nu$, where ν is the critical exponent defined by $\xi \sim |T - T_c|^{-\nu}$. Some exact inequalities among exponents were obtained by Schwartz and Soffer.[19] For the critical exponent η they found

$$\eta \geqslant \frac{4-d}{2} \tag{10}$$

and

$$\bar{\eta} \leqslant 2\,\eta. \tag{11}$$

In fact, it has been asserted[21–23] that $\bar{\eta} = 2\,\eta$ is an exact result.

Comparing Eqs. (6) and (7), one sees that

$$G(T,g) = \chi(T,g) + \sum_j [\langle \sigma_i \rangle_T \langle \sigma_j \rangle_T]_h . \tag{12}$$

Schwartz and Soffer[22] showed that with some assumptions, the second term in Eq. (12) is equal to $\beta^2 \chi^2 h_0^2$. If this were exact, then we would conclude that $G - \chi$ scales like χ^2, and hence that $\bar{\gamma} = 2\,\gamma$. Furthermore, this would also imply that[23]

$$A \equiv \lim_{T \to T_c^+(g)} \frac{G(T,g) - \chi(T,g)}{K^2 g \chi(T,g)^2} = 1. \tag{13}$$

However, recent work of Berger *et al.*[53] shows that in high dimensions, A is always finite and close, but not exactly equal, to unity. As discussed below, our series confirm the latter conclusion. The fact that A shows no tendency to diverge or vanish near T_c still implies that $\bar{\gamma} = 2\,\gamma$. Another exact inequality involves the critical exponent, α, for the divergence of the specific heat:[20]

$$2 - \alpha \leqslant \nu d - \gamma = \nu(d - 2 + \eta). \tag{14}$$

Next we turn to evaluations of the critical exponents. Roughly speaking there are two classes of theories. In the first of these classes one has so-called traditional "two-exponent scaling," in which a knowledge of two critical exponents (usually taken to be ν and η) determine all the other exponents. In the other class are theories which invoke a third independent exponent usually associated with a droplet picture. Many theories generate some version of dimensional reduction, in that hyperscaling relations (which involve the dimensionality) for the random field system contain the shifted value $(d - \theta)$ instead of d. If θ is not an independent exponent, then one has two-exponent scaling. However, the literature contains an open controversy concerning the exponent θ, which describes the singular part of the free energy, F_ξ, in a correlation volume: $F_\xi = F\xi^d \sim \xi^\theta$. ($F$ is the singular free energy per unit volume.) One can show[26–28] that $\theta = 2 - \bar{\eta} + \eta$. Therefore, if there are three independent exponents we may take the third one to be either θ or $\bar{\eta}$. The most important result of the present work, a brief summary of which was given previously,[54] is to establish that the critical point of the random field model is described by two-exponent scaling, through the relation $\bar{\eta} = 2\,\eta$.

The $d \to d-2$ dimensional reduction[8–10] was the first of the "two exponent" theories, since it implies a relation between η and $\bar{\eta}$, namely $\bar{\eta} = \eta$.[55] The discrepancy between $d_< = 2$ according to the Imry-Ma argument[6] and $d_< = 3$ according to the $d \to d-2$ dimensional reduction[8–10] in the Ising case led to a conjecture concerning θ already given in Ref. 8. It is maintained there that F_ξ behaves as $g\chi$. Since $\chi \sim \xi^{2-\eta}$, this ansatz leads to the relation $\theta = 2 - \eta$. The relation between θ and η implies again a two exponent picture, although now the relation between $\bar{\eta}$ and η is $\bar{\eta} = 2\,\eta$. The method of equivalent annealing, developed by Schwartz[21,30] yielded a modified dimensional reduction (explicitly considered for the exponent η), namely that the $d' = d - 2$ rule has to be replaced (at least for η) by

$$d' = d - 2 + \eta_0(d') = d - 2 + \eta(d), \tag{15}$$

where η_0 and η are the values of η for the system in zero random field and the random field system, respectively. The lower critical dimension turned out to be two and four for Ising and O(n) models, respectively, in accordance with Imry and Ma.[6] Theoretical arguments in favor of $\bar{\eta} = 2\,\eta$ are summarized in Ref. 23. As mentioned above, our results[54] support this suggestion. Subsequently Vojta and Schreiber[56] have analyzed a variant of the spherical model with long-ranged interactions $(J_{ij} \sim R_{ij}^{-s})$ and found $\bar{\eta}/2 = \eta = d + 2 - s$ for $d < s < d + 2$. (For $s > d + 2$, one has $\bar{\eta} = 2\,\eta = 0$.)

In contrast, an alternative approach[26–29] starts from a droplet picture and maintains that θ is a new independent

TABLE I. Critical exponents for the three-dimensional random field Ising model.

Method [a]	Ref.	γ	$\bar{\gamma}$	η	$\bar{\eta}$
Series	57	1.7			
Exact ground state	60				1.1
Domain-wall RG	62	1.58-1.60		0.5-0.72	
Real space RG	63	1.9-2.2			
Sim. DAFF	48			0.5 ± 0.1	1.0 ± 0.3
Sim.	47	1.7 ± 0.2		0.25 ± 0.03	0.8
Sim. Gaussian	50	1.7 ± 0.2	3.3 ± 0.6	0.50 ± 0.05	1.03 ± 0.05
Sim. bimodal	61	2.3 ± 0.3	4.8 ± 0.9	0.56 ± 0.03	1.00 ± 0.06
Series	This work	2.1 ± 0.2	4.2 ± 0.4		

[a]Sim. denotes simulation.

exponent, so that one needs three independent exponents to describe the critical behavior. For instance, Bray and Moore[27] derived scaling laws for the RFIM, based on the idea that the thermal phase transition is controlled by the zero-temperature fixed point. They showed that, except for hyperscaling, all the usual scaling laws of the pure Ising model applied to the random field case. They claimed that the number of independent exponents is three, that there is no dimensional reduction, and in particular, that their theory is inconsistent with the modified dimensional reduction of Eq. (15). However, they did calculate η and $\bar{\eta}$ in a $2+\epsilon$ expansion and found $\bar{\eta}=2\eta=2-\epsilon$, to all orders in ϵ. It was shown[30] that the modified dimensional reduction of Eq. (15) gives exactly the same result. Bray and Moore also found that hyperscaling is obeyed with the modified reduced dimension replacing d. Their claim of inconsistency with Eq. (15) is based on a calculation of ν in $2+\epsilon$ dimensions. Their calculation of ν depends on an unproved assumption. Indeed, a different assumption by Villain[26] leads to a different result for ν [and one which is also not consistent with Eq. (15)]. In any case, Bray and Moore[27] actually obtain (to all orders in ϵ) that the number of independent exponents is two. Continuing the ideas of Bray and MacKane,[24] Mezard and Young[25] have proposed a version of the ϵ expansion to take account of the multiple minima in the energy landscape of the random field model. Within a replica formalism they found an instability which has to be removed by replica symmetry breaking. This instability implies that the replica-symmetric fixed point, which leads to the usual ϵ-expansion result ($\bar{\eta}=\eta$), is unstable. Depending on the nature of the replica symmetry breaking, their theory gives $\bar{\eta}$ in the range $\eta<\bar{\eta}\leqslant 2\eta$. The result $\bar{\eta}=2\eta$ corresponds to maximal replica symmetry breaking and saturates the exact inequality $\bar{\eta}\leqslant 2\eta$.

There have been a number of attempts to obtain the critical exponents numerically and those results for $d=3$ which are most relevant to our work are summarized in Table I. Shapir and Aharony[57] derived and analyzed the seventh-order high-temperature series [i.e., in (J/T) and (H^2/T^2)] for the susceptibility of the RFIM on the FCC and general dimension hypercubic lattices. Besides verifying that $d_c=6$, they found (from the FCC series, which was the better behaved one) that $\gamma=1.7$ for $d=3$. Khurana *et al.*[58] and Houghton *et al.*[59,49] derived the seventh order series for the same quantity on a hypercubic lattice in general dimension as well. They expressed the series in terms of a series expansion in powers of (J/T) whose coefficients were given as explicit exactly evaluated functions of h_0/T. In principle, there should be a plateau region in g where the results are independent of g. However, their series were not long enough to obtain a recognizable plateau region. As a result, they did not obtain reliable estimates of the critical exponents for dimensions $d=3$ and $d=4$.

Monte Carlo simulations have been used to obtain critical exponents for the random field system, especially in three dimensions. As mentioned, Young and Nauenberg[47] attributed the fact that their exponents violated some of the exact bounds for a continuous transition to the fact that the transition was discontinuous. Ogielski and Huse[48] found a continuous transition for the bimodal distribution and gave $\eta=0.5\pm0.1$, and $\bar{\eta}=1.0\pm0.3$. Ogielski[60] obtained the critical behavior of the RFIM in three dimensions from correlation functions averaged over an ensemble of exact ground states. He found $\bar{\eta}\approx1.1$, $\nu\approx1.0$, and $\beta\approx0.05$. In work shortly after Ref. 54, Rieger and Young[50] carried out simulations which yielded both χ and G and obtained $\eta=0.60\pm0.03$ (or 0.56 ± 0.03) and $\bar{\eta}=0.97\pm0.08$ (or 1.00 ± 0.06) for $\beta h_0=0.25$ (or 0.35). Thus, although the results of Monte Carlo simulations (for similar values of g) suggested that perhaps $\bar{\eta}=2\eta$, at the time of this work[54] they were not yet completely convincing.[61]

The numerical domain-wall renormalization group analysis for the three-dimensional RFIM performed by Cheung[62] gave values of the critical exponents, some of which are listed in Table I. Dayan *et al.*[63] applied real space renormalization group (RG) analysis to the three-dimensional RFIM and obtained $1.9\leqslant\gamma\leqslant2.2$.

In view of this history, we decided to extend the high-temperature expansion. This extension became possible because of the existence of a tabulation of the weight factors (or the embedding constants) for arbitrary diagrams of up to 13 bonds on a hypercubic lattice.[64] Also, as we discuss in more detail below, we developed a number of algorithms to shorten the calculations. Normally, the determination of an exponent like η, which is not very large, is a difficult task. Here we took advantage of an aspect of the problem, not previously addressed by series, namely we focussed on testing the proposed relation $\bar{\eta}=2\eta$, which is equivalent to the relation $\bar{\gamma}=2\gamma$. This involved constructing (to our knowledge, for the first time) a series for the structure factor and comparing it with the series for the susceptibility. We were also able to construct a series for the amplitude ratio, A of

Eq. (13). The fact that we found[54] this ratio to be neither divergent nor vanishing as $T \to T_c$ indicates that $\bar{\eta} = 2\eta$. In addition, the value of A was found to be quite close to unity in all dimensions, as was suggested on theoretical grounds.[23] The purpose of this paper is to give the details of the construction of these series and their analysis, the results of which were summarized previously.[54] This avenue of research is presently continuing. Elsewhere[53] we will describe a study in high dimension which complements some of the results given here. In fact, the latter study led us to find an error in the last 2 terms of the series as reported in Ref. 54. The correct terms are given below, and all the series were reanalyzed yielding somewhat revised estimates for the exponents and amplitude ratio, as listed below. The corrections do not change the basic qualitative conclusions of Ref. 54.

Briefly, this paper is organized as follows. In Sec. II we discuss how the various series were constructed. In Sec. III we discuss briefly the way we analyzed the various series to get exponents and amplitude ratios. Data for the actual series coefficients are given in a set of Appendixes. Section IV contains a discussion of our results as a function of g and d. Here we obtain values of the exponents γ and $\bar{\gamma}$, alone and in combination, and also of the amplitude ratio A proportional to $(G-\chi)/\chi^2$. A discussion of these results is given in Sec. V.

II. FORMULATION

We have generated high temperature series for two quantities: the susceptibility χ and the structure factor G. The techniques used to generate these series, which are discussed below, represent an extension of those of Ref. 57.

A. Series for the susceptibility

To generate the susceptibility series, it is useful to relate it to the free energy. It is convenient to introduce various dimensionless or reduced quantities. For instance, we write the actual partition function $Z(K,\{\lambda_i\})$ in terms of a reduced partition function $Z^R(K,\{\lambda_i\})$ via $Z(K,\{\lambda_i\}) \equiv Z^R(K,\{\lambda_i\}) \times (\cosh K)^{N_B} \Pi_i [2\cosh(\beta h_i)]$, where the product is over all sites i and N_B is the total number of nearest–neighbor bonds in the lattice. Then

$$Z^R(K,\{\lambda_i\}) = \frac{1}{2^N} \mathrm{Tr} \left(\prod_{\langle i,j \rangle} (1 + w s_i s_j) \prod_i (1 + \tau_i s_i) \right), \tag{16}$$

where N is the total number of sites in the lattice, $w = \tanh \beta J$, $\tau_i = \tanh \lambda_i$, where $\lambda_i = \beta h_i$, and the trace is over $s_i = \pm 1$. Note that both w and τ_i can be easily expanded in powers of β starting with a term of order β. It is likewise convenient to define the reduced free energy (per site) in dimensionless form as $F^R(K,\{\lambda_i\}) = (1/N) \ln Z^R(K,\{\lambda_i\})$. Later on Z^R_Γ and $F^R_\Gamma(K,\{\lambda_i\})$ will denote the similarly defined reduced partition function and reduced free energy, respectively, of a system consisting of a set Γ of nearest-neighbor bonds. Also the susceptibility $\chi(T,g)$ and the reduced susceptibility, $\chi^R(T,g)$ obey

$$\chi(T,g) = (1/N) \sum_{i,j} [\partial^2 \ln Z(K,\{\lambda_i\})/(\partial \lambda_i \partial \lambda_j)]_h = (1/N) \sum_{i,j} [\partial^2 \ln Z^R(K,\{\lambda_i\})/(\partial \lambda_i \partial \lambda_j)]_h + [\mathrm{sech}^2 \lambda_i]_h$$

$$= \sum_{i,j} [\partial^2 F^R(K,\{\lambda_i\})/(\partial \lambda_i \partial \lambda_j)]_h + [\mathrm{sech}^2 \lambda_i]_h \equiv \chi^R(T,g) + [\mathrm{sech}^2 \lambda_i]_h . \tag{17}$$

Note that $[\mathrm{sech}^2 \lambda_i]_h$ does not depend on i, due to the configurational averaging. Clearly, since χ^R and χ differ only by a local quantity, they have the same critical properties. The diagrammatics naturally produce a series for $\chi^R(T,g)$ which we then convert into a series for $\chi(T,g)$ using the above.

Because $s_i^2 = 1$ we may write Z^R in the form

$$Z^R(K,\{\lambda_i\}) = \sum_{n=0}^{\infty} \sum_{C_n} \left(\prod_{i \in SC_n} \tau_i \right) w^n, \tag{18}$$

where C_n is a configuration of n bonds on the lattice and SC_n is the set of end points of those bonds that are common to an odd number of bonds belonging to the configuration. Then the reduced free energy is given by

$$F^R(K,\{\lambda_i\}) = \frac{1}{N} \sum_{n=1}^{\infty} \sum_{\Gamma_n} \phi_{\Gamma_n}(K,\{\lambda_i\}), \tag{19}$$

where the sum over Γ_n is over all *connected* diagrams having n bonds and $\phi_{\Gamma_n}(K,\{\lambda_i\})$ is the weight associated with Γ_n. This weight is simply the cumulant free energy associated with the set of bonds of Γ:

$$\phi_\Gamma(K,\{\lambda_i\}) = F^c_\Gamma(K,\{\lambda_i\}), \tag{20}$$

where the cumulant (indicated by the superscript "c") is defined recursively via

$$F^c_\Gamma(K,\{\lambda_i\}) = F^R_\Gamma(K,\{\lambda_i\}) - \sum_{\gamma \subset \Gamma} F^c_\gamma(K,\{\lambda_i\}), \tag{21}$$

where the sum is over sets of bonds γ which represent proper subsets of the bonds of Γ ($\gamma = \Gamma$ is not allowed). From the property of cumulants (i.e., that F^c_Γ vanishes if any bond, K in Γ is set equal to zero), one can show that the series expansion of F^c_Γ in powers of K begins at order K^p, where p is the number of bonds in Γ. Note that ϕ depends on the position and orientation of the diagram on the lattice through its

dependence on the local fields λ_i. Thus the sum in Eq. (19) counts separately diagrams which differ only in their location and/or orientation on the lattice.

The reduced susceptibility is given by

$$\chi^R(T,g)=\sum_{n=1}^{\infty}{\sum_{\Gamma_n}}' W(\Gamma_n)\sum_{i,j}\left[\partial^2 F^c_{\Gamma_n}(K,\{\lambda_i\})/(\partial\lambda_i\partial\lambda_j)\right]_h, \tag{22}$$

where Σ' denotes that the summation here is only over topologically distinct diagrams and $W(\Gamma_n)$ is the weak embedding constant which gives the number of ways per site a diagram topologically equivalent to Γ can be embedded in an infinite lattice. (Two diagrams are topologically equivalent to one another if their sites can be relabeled so that they both have the same nearest neighbor bonds. Thus all self-avoiding walks of length n are topologically equivalent to one another.) After the average over the distribution of random fields it is no longer necessary to sum separately over topologically equivalent diagrams.

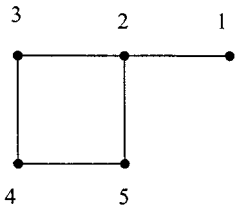

FIG. 2. A diagram for the high-temperature series.

To clarify our approach, we discuss the calculations for the diagram Γ shown in Fig. 2. The reduced partition function for that diagram is given by

$$\begin{aligned}Z^R_\Gamma(K,\{\lambda_i\})]=1&+w(\tau_1\tau_2+\tau_2\tau_3+\tau_3\tau_4+\tau_2\tau_5+\tau_4\tau_5)+w^2(\tau_1\tau_3+2\,\tau_2\tau_4+\tau_1\tau_5+2\,\tau_3\tau_5+\tau_1\tau_2\tau_3\tau_4+\tau_1\tau_2\tau_4\tau_5\\&+2\,\tau_2\tau_3\tau_4\tau_5)+w^3(\tau_2\tau_3+2\,\tau_1\tau_4+\tau_3\tau_4+\tau_2\tau_5+\tau_4\tau_5+2\,\tau_1\tau_2\tau_3\tau_5+2\,\tau_1\tau_3\tau_4\tau_5)+w^4(1+\tau_1\tau_3+\tau_1\tau_5\\&+\tau_1\tau_2\tau_3\tau_4+\tau_1\tau_2\tau_4\tau_5)+w^5\tau_1\tau_2.\end{aligned} \tag{23}$$

Next we expand F^R_Γ in powers of w. Eventually we want to obtain a series up to, say, pth order in K for $[\partial^2 F^R_\Gamma/(\partial\lambda_i\partial\lambda_j)]_h$. The following points which simplify the calculation should be noted.

(a) The highest order needed in the expansion of F^R_Γ in w is clearly p.

(b) As a result of the expansion of F^R_Γ we obtain a polynomial in w with coefficients which are polynomials in the τ_i's. Since each τ_i carries at least one factor of $\lambda_i=\beta h_i$, one sees that (keeping in mind that two derivatives with respect to λ are needed) the total number of τ_i's plus the power of w in a term should not exceed $p+2$.

(c) Furthermore, there is a part of the series that vanishes when all the fields are set to zero. In that part the lowest order contribution to τ_i is λ_i. The process of averaging will yield a nonzero result if λ_i appears in the product, after taking the second derivative, an even number of times. Therefore, each term that vanishes with g in the coefficient of w^n carries at least a factor K^2 coming from the τ's, so that if we are interested only in expanding to order p in K, the coefficients of w^{p-1} and w^p can be taken with $g=0$. Thus the coefficients of w^{p-1} and w^p are those of the pure system.

We proceed now to calculate F_Γ from Eq. (23). Since its expansion is quite complicated, and since we are interested in showing the simplifications obtainable by deleting terms that do not survive ''averaging,'' we consider A_4, the coefficient of w^4, and work up to order K^7. (By ''averaging'' we mean taking two derivatives with respect to the λ_i's and then averaging over the distribution of random fields.)

We find that

$$\begin{aligned}A_4=1&+\tau_1\tau_3-\tau_1{\tau_2}^2\tau_3-\frac{{\tau_1}^2{\tau_3}^2}{2}-{\tau_2}^2{\tau_3}^2-2\,{\tau_1}^2\tau_2\tau_4-4\,\tau_1\tau_2\tau_3\tau_4-2\,\tau_2{\tau_3}^2\tau_4-2\,{\tau_2}^2{\tau_4}^2-2\,\tau_1\tau_3{\tau_4}^2-{\tau_3}^2{\tau_4}^2+\tau_1\tau_5\\&-\tau_1{\tau_2}^2\tau_5-{\tau_1}^2\tau_3\tau_5-2\,{\tau_2}^2\tau_3\tau_5-2\,\tau_1{\tau_3}^2\tau_5-4\,\tau_1\tau_2\tau_4\tau_5-8\,\tau_2\tau_3\tau_4\tau_5-2\,\tau_1{\tau_4}^2\tau_5-2\,\tau_3{\tau_4}^2\tau_5-\frac{\tau_1 2{\tau_5}^2}{2}-{\tau_2}^2{\tau_5}^2\\&-2\,\tau_1\tau_3{\tau_5}^2-2\,{\tau_3}^2{\tau_5}^2-2\,\tau_2\tau_4{\tau_5}^2-{\tau_4}^2{\tau_5}^2.\end{aligned} \tag{24}$$

In the above expression we have already deleted terms with six or more τ's, since such terms would contribute to order K^8 and higher. Now, terms in Eq. (24) that contain more than two odd powers of τ_i's, such as

$$\tau_1\tau_2\tau_3\tau_4 \tag{25}$$

in the last expression, give zero contribution after ''averaging.'' Also, terms which only differ by labeling of variables, for example

$$\tau_1{\tau_4}^2\tau_5,\ \tau_1\tau_3{\tau_5}^2 \tag{26}$$

give the same contribution after ''averaging.'' We tabulate all the different combinations of τ's that give nonzero contribution. For instance,

$$t_1=\tau_i\tau_j,\ \ t_2=\tau_i^2\tau_j\tau_k,\ \ t_3=\tau_i^2\tau_j^2,\ \ \text{etc.}, \tag{27}$$

with $i\neq j\neq k\neq\ldots$. The full list of t_i's can be found in Appendix A. Thus, Eq. (24) becomes

$$A_4 = 1 + 2\,t_1 - 21\,t_2 - 9\,t_3 \tag{28}$$

and

$$\sum_{i,j} [\partial^2 A_4/(\partial\lambda_i \partial\lambda_j)]_h = 4([d\tau_i/d\lambda_i]_h)^2 - 42[\tanh^2\lambda_i]_h([d\tau_i/d\lambda_i]_h)^2 - 18[\tanh^2\lambda_i]_h[d^2\tau_i^2/d\lambda_i^2]_h . \tag{29}$$

All the quantities appearing here can easily be calculated given the distribution of random fields and then a series expansion in powers of β can be constructed. Therefore, the problem is reduced to the identification of the t_i's and calculation of the number of times each t_i appears in the expansion of F from each diagram.

The main problem now is how to construct an automatic procedure to evaluate F_Γ for an arbitrary diagram Γ. We note that for any diagram we can write Z_Γ in a form that is illustrated by the following expression, for the 5-bond diagram:

$$Z_\Gamma = 1 + wc(1,2) + w^2[c(2,2)+c(2,4)] + w^3[c(3,2)+c(3,4) + c(3,6)] + w^4[c(4,0)+c(4,2)+c(4,4)] + w^5 c(5,2), \tag{30}$$

where in $c(m,n)$ m is the power of w and n denotes the number of τ's. It should be noted that $c(m,n)$ is the sum of all terms with a given number of τ's and as such it is a function of the τ's that depends on the specific diagram. For instance for the diagram shown in Fig. 2, we have

$$c(2,4) = \tau_1\tau_2\tau_3\tau_4 + \tau_1\tau_2\tau_4\tau_5 + 2\,\tau_2\tau_3\tau_4\tau_5 . \tag{31}$$

The point is that we can write down directly the power series in w for F_Γ in terms of the $c(m,n)$'s. Now we obtain

$$F_\Gamma = wc(1,2) + w^2\left(\frac{-c(1,2)^2}{2} + c(2,2) + c(2,4)\right) + w^3\left[\frac{c(1,2)^3}{3} - c(1,2)c(2,2) - c(1,2)c(2,4) + c(3,2) + c(3,4) + c(3,6)\right] + w^4\left[\frac{-c(2,2)^2}{2} - c(1,2)c(3,2) + c(4,0) + c(4,2) + c(4,4)\right] + w^5[-c(2,2)c(3,2) - c(1,2)c(4,0) - c(1,2)c(4,2) + c(5,2)]. \tag{32}$$

This result looks simpler than the terms of order w^4 for A_4 given in Eq. (24), because it is written in terms of the $c(m,n)$'s that are functions of the τ's. The expression may be further simplified by deleting all those terms that will obviously not survive "averaging." First, terms where the $c(m,n)$'s appear linearly in F_Γ with n exceeding two must vanish after "averaging." The reason is that each of the $c(m,n)$'s viewed as a function of one of the τ's, say τ_1, is a monom. Namely, it is of the form $A + B\tau_1$, where A and B do not depend on τ_1 but only on the other τ's. Also, a product $\Pi_i c(m_i,n_i)$ must vanish after "averaging" if $s \equiv n_k - \Sigma_{i\neq k} n_i > 2$, where n_k is the maximal n. (The quantity $s-2$ is the minimum number of monoms which must remain after two derivatives with respect to the random field are taken.) After deleting the terms discussed above, we obtain

$$F_\Gamma^R = wc(1,2) + w^2\left[\frac{-c(1,2)^2}{2} + c(2,2)\right] + w^3\left[\frac{c(1,2)^3}{3} - c(1,2)c(2,2) - c(1,2)c(2,4) + c(3,2)\right] + w^4\left[\frac{-c(2,2)^2}{2} - c(1,2)c(3,2) + c(4,0) + c(4,2)\right] + w^5[-c(2,2)c(3,2) - c(1,2)c(4,0) - c(1,2)c(4,2) + c(5,2)]. \tag{33}$$

This result is much simpler than that of Eq. (32). In the last stage the t's in the function of the specific c's for each diagram are identified and then after taking the second derivative with respect to λ_i and λ_j each expression is replaced by its average to the required order of K.

There were two stages of code development. At first the MATHEMATICA program that goes through all the stages described above, was developed. The weakness of the MATHEMATICA program is that it is too slow when an actual calculation of the contribution of a diagram is performed. Namely in that part where the specific c's have to be multiplied out, written as a function of the τ's, t's are to be identified and replaced by the proper averages. Therefore, a FORTRAN program has been written to speed up the calculations. The main idea is to introduce an array of 15 columns for each $c(m,n)$. Each row (of length 15) contains ones and zeros and stands for a given product of τ's. (Remember that each product either contains a given τ or not.) The first number in each row shows the number of identical products. This enables simple manipulations with the $c(m,n)$'s in a FORTRAN integer program. The fact that we have two different programs that perform equivalent calculations provides us with a powerful checking tool, that was used on a number of high order diagrams. The actual series for the susceptibility are given in Appendixes C and E for the Gaussian and bimodal distributions, respectively.

B. Series for the structure factor

The calculation of G involves the calculation of the correlation function

$$G(k,l)\equiv\langle s_k s_l\rangle_T=\frac{\mathrm{Tr}(s_k s_l\Pi_{\langle i,j\rangle}(1+ws_is_j)\Pi_i(1+\tau_i s_i))}{\mathrm{Tr}(\Pi_{\langle i,j\rangle}(1+ws_is_j)\Pi_i(1+\tau_i s_i))}\equiv\frac{N(k,l)}{D}. \tag{34}$$

In principle, the correlation function can also be obtained by adding the interaction $-\mu_{kl}s_k s_l$ to the dimensionless Hamiltonian ($\beta\mathscr{H}$) and then taking the derivative of the free energy (19) with respect to μ_{kl}:

$$\langle s_k s_l\rangle_T=\frac{\partial}{\partial\mu_{kl}}F(\mu_{kl})\bigg|_{\mu_{kl}=0}. \tag{35}$$

Therefore, we conclude that only connected diagrams will contribute to Eq. (34). Furthermore the contribution from each connected diagram can be calculated by taking the cumulant just as we did for the susceptibility. In actuality we used Eq. (34) to evaluate $G(k,l)$. Consider first the numerator of this expression. It is a polynomial in w with coefficients that are polynomials in the τ's and that are monoms for each τ separately. The numerator on a five bond diagram, for example, is generally written as

$$N_\Gamma(k,l)=\mathrm{Tr}\left(s_k s_l\prod_{\langle i,j\rangle}(1+ws_is_j)\prod_i(1+\tau_i s_i)\right)=s(0,2)+w[s(1,0)+s(1,2)+s(1,4)]+w^2[s(2,0)+s(2,2)+s(2,4)]$$
$$+w^3[s(3,0)+s(3,2)+s(3,4)+s(3,6)]+w^4[s(4,0)+s(4,2)+s(4,4)+s(4,6)]+w^5[s(5,0)+s(5,2)+s(5,4)]. \tag{36}$$

Here the $s(m,n)$'s are the analogs of the $c(m,n)$'s appearing in the calculation of the partition function and of course depend on the diagram. A specific example for the diagram Γ of Fig. 2 is

$$N_\Gamma(2,3)=\tau_2\tau_3+w(1+\tau_1\tau_3+\tau_2\tau_4+\tau_3\tau_5+\tau_2\tau_3\tau_4\tau_5)+w^2(\tau_1\tau_2+\tau_1\tau_4+2\,\tau_3\tau_4+2\,\tau_2\tau_5+\tau_1\tau_2\tau_3\tau_5+2\,\tau_4\tau_5+\tau_1\tau_3\tau_4\tau_5)$$
$$+w^3(1+\tau_2\tau_4+2\,\tau_1\tau_2\tau_3\tau_4+2\,\tau_1\tau_5+\tau_3\tau_5+2\,\tau_1\tau_2\tau_4\tau_5+\tau_2\tau_3\tau_4\tau_5)+w^4(\tau_1\tau_2+\tau_2\tau_3+\tau_1\tau_4+\tau_1\tau_2\tau_3\tau_5$$
$$+\tau_1\tau_3\tau_4\tau_5)+w^5\tau_1\tau_3. \tag{37}$$

Next we expand the numerator over the denominator as a polynomial in w with coefficients that are functions of the $c(m,n)$'s and the $s(m,n)$'s. In this procedure we already discard terms that will not contribute to the desired order in K. The simplification procedure and identification of terms that will contribute to the average is much the same as in the previous section. The corresponding list of contributing τ products is given in Appendix B.

The actual series for the structure factor are given in Appendixes D and F for the Gaussian and bimodal distributions, respectively.

C. Series for the pure Ising model in general dimension

As described in the previous sections, the g-dependent coefficients contribute only up to order $(p-2)$ in the expansion to order p in K. The $(p-1)$th and pth order come from the expansion of the pure system. Therefore, we required a fifteenth order expansion in K of the pure system for general d. We have constructed this expansion up to order K^{15} using the method proposed by Harris[65] which uses only the no-free-end (NFE) diagrams. Although the calculations for each diagram are somewhat more complicated than in the traditional method, the amount of computer time saved is large because there are very many fewer diagrams. For instance, the total number of diagrams with at most 13 bonds on a hypercubic lattice is 20724, whereas the number of the NFE diagrams with 15 bonds is only 842. The occurrence factors (weak embedding constants) for these diagrams are given for general dimension in Ref. 66.

The application of this method for the calculation of the susceptibility of the Ising model is given in Refs. 65 and 67. There the result is written as

$$\chi=(1+t)\chi_0+\sum_\Gamma w(\Gamma)\chi^c(\Gamma), \tag{38}$$

where $\chi_0=(1-\sigma t)^{-1}$, $\sigma=2d-1$, and the superscript "c" indicates the cumulant. The cumulant is recursively defined by Eq. (21). Here the bare susceptibility, $\chi(\Gamma)$ is defined to be

$$\chi(\Gamma)=\chi_0^2\left[t^2\sum_i z_i(\Gamma)^2-2n_b(\Gamma)t(1+t)\right]$$
$$+2\sum_{i<j\in\Gamma}\gamma_i(\Gamma)\gamma_j(\Gamma)\chi_{ij}(\Gamma), \tag{39}$$

where $z_i(\Gamma)$ is the number of sites in Γ which are constrained to be nearest neighbors of site i. Also $\gamma_i(\Gamma)=1+[z-z_i(\Gamma)]t\chi_0$ and $\chi_{ij}(\Gamma)$ is the two-point susceptibility of the cluster Γ:

$$\chi_{ij}(\Gamma)=\frac{\mathrm{Tr}\{\sigma_i\sigma_j\exp[\beta J\Sigma_{\langle kl\rangle\in\Gamma}\sigma_k\sigma_l]\}}{\mathrm{Tr}\{\exp[\beta J\Sigma_{\langle kl\rangle\in\Gamma}\sigma_k\sigma_l]\}}. \quad (40)$$

Besides usual internal checks like cumulant subtraction, the final check was a comparison with existing series for square[68] and simple cubic lattices[69] as well as with some earlier results in higher dimensions.[70] Our results also agree with a previous work[71] specialized to 5 and 6 dimensions which was based on the same tabulation of diagrams. These results were reported and analyzed elsewhere[72,73] without any derivation.

III. ANALYSIS METHODS

In this section we describe briefly some of the methods of analysis used in this work. The three series presented above are expected to take the form[74]

$$f(x)\sim A(1-x/x_c)^{-\gamma}\{1+A_1(1-x/x_c)^{\Delta_1}+A_2(1-x/x_c)^{\Delta_2}+\cdots\}, \quad (x\to x_c), \quad (41)$$

except at the upper critical dimension, where the right-hand side may involve logarithmic corrections.[75] In all our methods we approximate a function of interest, $h(x)$, by the Padé approximant[76] $[L/M]$:

$$h(x)\sim\frac{P_L(x)}{Q_M(x)}=[L/M]=\frac{p_0+p_1x+\cdots+p_Lx^L}{1+q_1x+\cdots+q_Mx^M}. \quad (42)$$

The coefficients of the polynomials P and Q are chosen so that the expansion of $h(x)$ to order $N=L+M$ agrees with the corresponding expansion of the approximant $[L/M]$. For example, if $f(x)$ has an assumed singularity of the form $f(x)\sim A(1-x/x_c)^{-\gamma}$ then the Dlog Padé analysis considers the function $h(x)=d\ln f(x)/dx$. The function $h(x)$ presumably has a simple pole at $x=x_c$ with residue $-\gamma$. Since it is expected to be a rational function, $h(x)$ is reasonably represented by the $[L/M]$ approximant of Eq. (42). Accordingly, the location of the physical pole and the residue of the $[L/M]$ Padé approximant provide estimates for the desired quantities, x_c and γ. We also used two other methods, $M1$ and $M2$, which we now describe briefly.[77,78]

The M1 method. This works best when Δ_1 is close to 1. We approximate $f(x)$ by

$$A(1-x/x_c)^{-\gamma}[1+A_1(1-x/x_c)^{\Delta_1}], \quad (43)$$

and construct a function

$$H(x)=\gamma f(x)-(x_c-x)\frac{df}{dx}, \quad (44)$$

whose critical behavior is of the form

$$H(x)\sim B\left(1-\frac{x}{x_c}\right)^{-\gamma+\Delta_1}, \quad (45)$$

where $B=\Delta_1AA_1$. For trial values of x_c and γ we obtain the corresponding Δ_1 from a Padé approximant $[L/M]$ to $(d/dx)\ln H(x)$. Changing the trial value of x_c gives surfaces in the (x_c,γ,Δ_1) space, each surface corresponding to a different $[L/M]$ Padé approximant. The correct estimate of (x_c,γ,Δ_1) will be given by the intersection point of all these surfaces.

The M2 method. In the $M2$ method one first transforms the series $f(x)=\Sigma_n a_nx^n$ into a series in the variable[79]

$$y=1-\left(1-\frac{x}{x_c}\right)^{\Delta}, \quad (46)$$

where Δ is now an adjustable parameter. We then derive a series for

$$F_\Delta(y)=\Delta(1-y)\frac{d}{dy}\ln f(x(y))=\gamma-\frac{A_1\Delta_1(1-y)^{\Delta_1/\Delta}+\cdots}{1+A_1(1-y)^{\Delta_1/\Delta}+\cdots}, \quad (47)$$

where the higher confluent corrections have been dropped. Now γ is calculated as a function of Δ using different Padé approximants to $F_\Delta(y)$ at $y=1$. This construction yields a family of $\gamma(\Delta)$ curves in the (γ,Δ) plane and $\gamma(\Delta,x_c)$ surfaces in the (x_c,Δ,γ) space. The correct estimate of (x_c,Δ_1,γ) is given by the intersection point of all these surfaces. Note that when $\Delta=1$ we recover the usual Dlog Padé method.

In what follows, we replace x and x_c by K and K_c. The analysis of series at fixed values of d and g proceeds as follows. At first we use the conventional Dlog Padé analysis to select a region in the (K_c,γ) space for closer analysis. Then, within this region, we run the $M1$ and $M2$ routines which prepare the data for five trial values of K_c (five slices) using 10–15 of the highest Padé approximants for several hundred input values of γ or Δ_1. There are two graphical routines which produce the output. The first one provides three-dimensional graphics for all the five slices,[78] whereas the second one draws a two-dimensional plot for the central value of temperature (the central slice). It is useful to use the two methods in conjunction with one another: both methods should lead to the same values of the exponents. To illustrate these analyses, we now show some examples and explain in detail the conclusions that we draw from the graphs. Figures 3 and 4 show plots from methods $M1$ and $M2$, respectively, for the susceptibility series at $g=10$ and the Gaussian distribution for $d=8$. For $d>6$, theory predicts that $\gamma=1$ and $\Delta_1=(d-6)/2$. Looking at the graphs, one can locate a point of intersection (i.e., a point from which curves emanate in various directions) in each plot. In test series, this is always very clear. In real systems, this point is sometimes less clearly identified. Sometimes one finds more than one intersection region in one of the analyses. In such cases, we use the degree to which $M1$ and $M2$ give consistent values for the exponents as an indication for the uncertainty in the results. There are also some rule-of-thumb features that recur frequently and aid in our deductions. In the $M1$ method, Fig. 3, we can see that in plot 3(a), drawn at a trial K_c value of 0.070 653 14, there is a nice intersection region at $\gamma=1.002\pm0.003$ and $\Delta_1=0.95\pm0.15$. The convergence region is indicated by a box in the figure, and the estimates are in pleasing agreement with the exact values of 1 for both exponents. As we reduce the K_c value very slightly, to $K_c=0.070\,645\,62$, we see that the $M1$ intersection region in

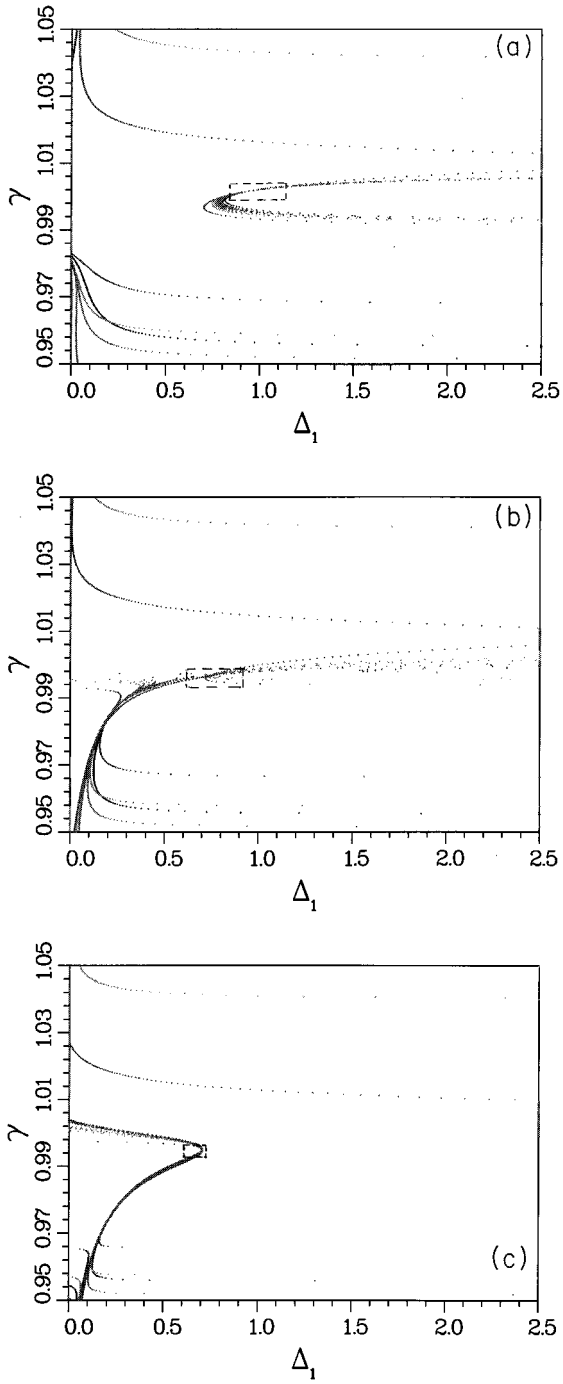

FIG. 3. $M1$ analysis of the $d=8$, $g=10$ Gaussian distribution susceptibility series. (a) $K_c=0.070\ 653\ 14$; (b) $K_c=0.070\ 645\ 62$; (c) $K_c=0.070\ 638\ 10$.

plot 3(b) is far more symmetrical with curves facing all directions, not merely to the right of the figure. In plot 3(c), at $K_c=0.070\ 638\ 10$, the curves face leftwards. This change of curve direction in $M1$ graphs is one rule of thumb used to identify the correct critical point (for example, it occurs in the exactly soluble Baxter-Wu model[78] at the exact critical point), but here the best exponent values are seen in plot 3(a), while the central exponent estimates deduced from 3(b) and 3(c) are slightly lower. We conclude that the best estimates for K_c lie between 3(a) and 3(b), and include the difference in the errors. In this case, since $\Delta_1=1$, experience

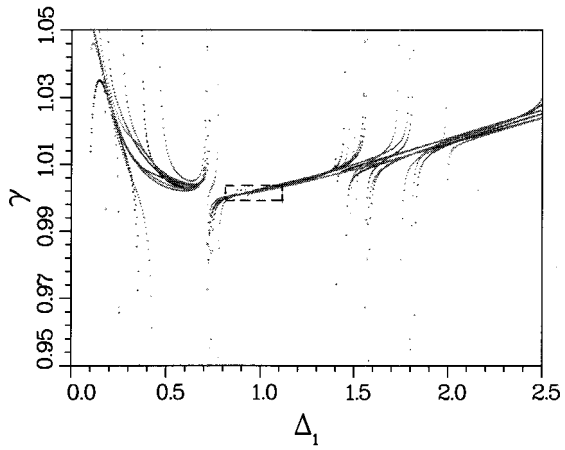

FIG. 4. $M2$ for same series as in Fig. 3, at $K_c=0.070\ 653\ 14$.

shows that the $M1$ analysis is of a superior quality to the $M2$. The $M2$ curve at $K_c=0.070\ 653\ 14$, shown in Fig. 4, gives consistent results for comparison purposes. If we overlap the plots 3(a) and 4 we find that the two intersection points overlap, giving $\gamma=\Delta_1=1$. Since the best numbers are seen just a little above the crossover point, this gives us an idea of the error induced by the finite length of our series. Overall we deduce $K_c=0.070\ 646\pm0.000\ 010$ for this case.

A representative plot of data from a lower dimension is given in Fig. 5, where we illustrate the $M1$ and $M2$ analyses

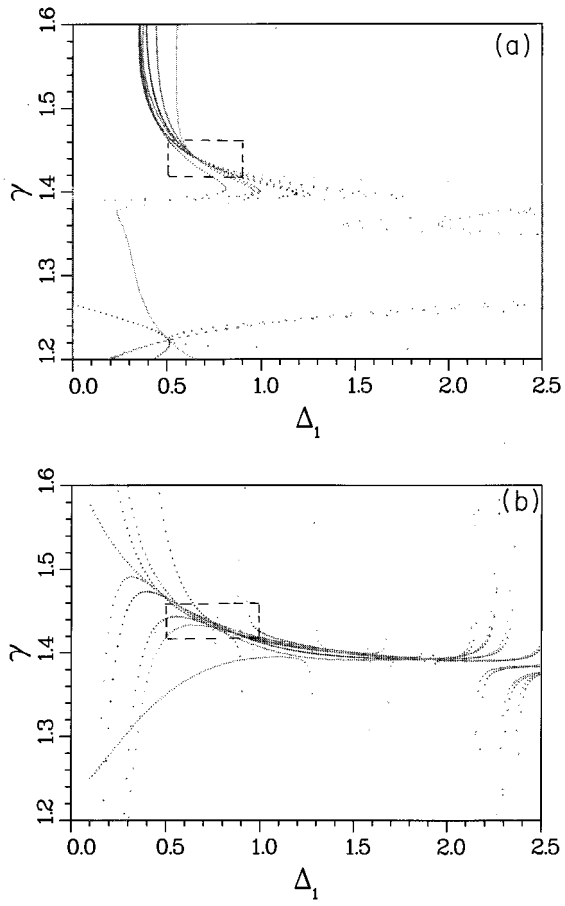

FIG. 5. Analysis of the $d=4$, $g=6$ Gaussian distribution, at $K_c=0.1894$. (a) $M1$; (b) $M2$.

in Figs. 5(a) and 5(b), respectively, for $d=4$, $g=6$ and a Gaussian distribution at $K_c=0.1894$. In the former, we see a clear intersection near $\gamma=1.44$ and $\Delta_1=0.7$. In the latter there is a broader intersection region, spread out over $1.46>\gamma>1.42$ and $0.5<\Delta_1<1.0$, but sharpening near $\Delta_1=0.8$, and a very fine one at $\gamma=1.4$ and $\Delta_1=1.7$. Since only one region is common to both methods, and the leftmost region is the correct one in test-series where both regions do not give the same dominant exponent, we conclude here that $\gamma=1.44\pm0.02$ and $\Delta_1=0.7\pm0.2$ for this temperature choice.

For $d>6$ the series gave a sufficiently clear confirmation of the mean field values of the exponents, so that we used the $M1$ and $M2$ methods directly. For lower d, to obtain results for exponents and for the amplitude ratio A of Eq. (13) we proceeded in four stages. We assume that Eqs. (8) and (9) describe the asymptotic behavior of χ and G, respectively, near the critical point at $T_c(g)$. Universality implies that γ and $\bar{\gamma}$ are independent of g over the range of g in which the transition remains continuous. However, the finite series usually lead to parameter–dependent exponents (see, e.g., Ref. 57).

In the first stage of analysis our goal was to find a range of g, where this dependence of the exponents on g is very weak. For the purpose of defining this range in g, we found it convenient to use a method of estimating the critical exponents which avoided the uncertainties associated with the fact that we did not have a precise determination of $K_c(g)$. Accordingly, we used a Dlog Padé analysis of series obtained from term-by-term division[80,81] of the coefficients of the series for G by those of χ. By term-by-term divided series we mean the following. Suppose the series for χ and G are given by $\chi=\Sigma a_i K^i$ and $G=\Sigma b_i K^i$, respectively. Then we define the term by term divided series, $[G/\chi]$ by

$$[G/\chi]\equiv\sum \frac{b_i}{a_i}x^i\sim(1-x)^{-(\bar{\gamma}-\gamma+1)}. \tag{48}$$

An advantage of this analysis is that as long as χ and G diverge at the same point, the term-by-term divided series diverge at $x=1$. The resulting approximate estimates for $(\bar{\gamma}-\gamma)$ showed a very rapid increase (at $g<0.1$) from zero (at $g=0$) to values of $(\bar{\gamma}-\gamma)$ which are close to estimates of γ found by later direct analyses (see below). As g is increased further, $(\bar{\gamma}-\gamma)$ exhibits a very slow increase, over a wide range in g. This range, which is almost a plateau, is much larger than observed before with the much shorter series.[57,49] At still larger $g>g_1$ we saw a second crossover, with an apparent rapid increase in $(\bar{\gamma}-\gamma)$. We have thus concentrated on the "plateau" region. It should be emphasized that the term-by-term divided analysis was used just to obtain a rough estimate of $(\bar{\gamma}-\gamma)$ and the plateau region.

TABLE II. Values of critical exponent γ obtained from series.

d	γ
8	1.00 ± 0.01
5	1.13 ± 0.03
4	1.45 ± 0.05
3	2.1 ± 0.2

In the second stage, we combined recently developed efficient visualization methods[78] with the $M1$ and $M2$ algorithms (see above) to study series for χ and G in the above g windows. We obtained the critical values $K_c(g)$ and values of the exponents, at selected g values in different dimensions. We give a discussion for each dimension below.

In the third stage, we addressed the issue of two versus three independent exponents,[54] by studying the amplitude ratio, A of Eq. (13). To evaluate A we obtained Padé approximants for Eq. (13) at $K_c(g)$ (as obtained above). As found in other studies,[82,83] the Padé estimate of such ratios, which involve only amplitudes on the same side of the transition, are very stable to errors in K_c and to correction terms. We found that A also exhibited a "plateau" in g which was even flatter than that found for the difference $(\bar{\gamma}-\gamma)$ mentioned above. The value of A was always close to unity. As already stated, the fact that A neither diverges nor vanishes near K_c implies that $\bar{\gamma}=2\gamma$.

In the final stage, we deduced overall exponent estimates. Having identified the range of g values for which A is practically constant (Gaussian distribution), or varies slowly (bimodal case), we looked back at the values of γ and $\bar{\gamma}$, measured at the second stage. The series for G contain more correction terms [arising from corrections to Eq. (13) (Ref. 22)] and generally behave less well than those for χ. Given our result that $A\approx1$, we consider it established that $\bar{\gamma}=2\gamma$, and therefore we will quote only values for γ. Eventually, we averaged over the gradual increase in the exponents with g, and included the appropriate range in the error bars. The final estimates are summarized in Table II.

IV. RESULTS FROM ANALYSIS OF SERIES

A. Above six dimensions

Mean field theory predicts that above the upper critical dimension $d_>=6$ one has $\bar{\gamma}=2\gamma=2$ and $\Delta_1=(d-6)/2$. We started by checking this relation for $d>6$. Since the series behaved quite well, we used the $M1$ and $M2$ methods of analysis, as illustrated in Figs. 3 and 4 and as discussed in the previous section. Similar analyses over a range of g values led us to the overall results

$$\gamma=1\pm0.01,\quad \bar{\gamma}=2\pm0.01,\quad \Delta_1=1.0\pm0.2 \tag{49}$$

TABLE III. Values of the amplitude ratio A [Eq. (13)] for $d=8$, $g=10$.

		$d=8$, $g=10$					
			Values of Padé approximants for A				
g	Distribution	K_c	[7/6]	[6/7]	[6/6]	[5/6]	[6/5]
10	Gaussian	0.0706375	1.00171	1.00171	1.00176	1.00167	1.00167
10	Bimodal	0.070865	1.06787	1.06808	1.06771	1.06773	1.06773

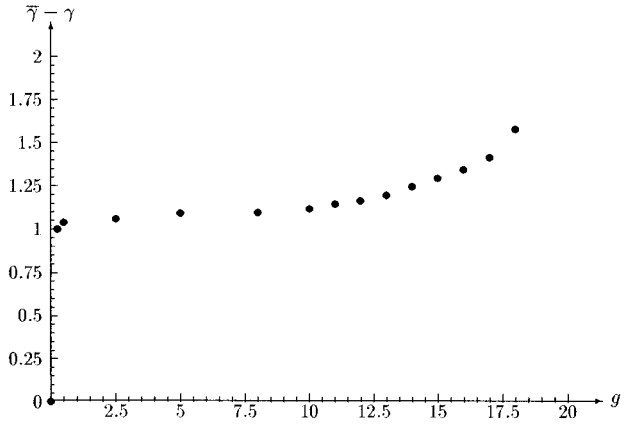

FIG. 6. Term-by-term divided series. Gaussian distribution. $d=5$.

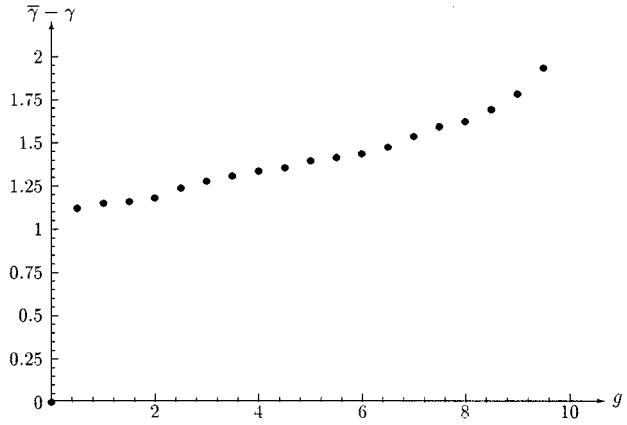

FIG. 8. Term-by-term divided series. Gaussian distribution. $d=4$.

for both Gaussian and bimodal distributions at $d=8$, in agreement with theoretical expectations. Some values of K_c and the amplitude ratio, A, are presented in Table III. The comparison of these values with the $1/d$ expansion will be given elsewhere.[53]

B. Five and four dimensions

We commence with the results of the biased Dlog Padé analysis of the term-by-term divided series for the two distributions of random fields in Figs. 6 and 7 for $d=5$ and in Figs. 8 and 9 for $d=4$. We deduce that the "plateau" region (the region between g-small and g-large crossovers) is $0.1<g<15$ $(0.1<g<6)$ for the Gaussian distribution, and $0.1<g<10$ $(0.1<g<4)$ for the bimodal distribution for $d=5$ $(d=4)$. Tables IV and VI present the results of the $M1$ and $M2$ analysis of the χ and G series. We observe that the values of $\bar{\gamma}-\gamma$ obtained from the independent analysis of the χ and G series are in accord with the values of $\bar{\gamma}-\gamma$ obtained from the term-by-term divided series, Eq. (48). Tables V and VII exhibit several near-diagonal high-order approximants for A for both distributions. Our final estimates for the critical exponent γ are given in Table II.

C. Three dimensions

The analysis of the three dimensional series was somewhat more complicated than that at higher dimensions. Initially, as above, the "plateau" region was established (see Figs. 10, 11). We found the "plateau" as $0.1<g<1.0$ for both distributions. A similar plateau was found for the amplitude ratio A and data for this region is given in Table VIII. Preliminary analysis of 13 terms of the χ and G series indicated a divergence with the same exponent for both quantities. Note that for $d=3$ the plateau occurs for smaller values of g than in higher dimension. Also, from Eq. (12) one obtains

$$G=\chi+gK^2\chi^2+\cdots. \tag{50}$$

Thus for small gK^2, the two quantities G and χ are nearly the same until one gets quite close to the critical point where all the quantities diverge. To overcome this problem we constructed $G-\chi$, divided out gK^2, and analyzed the resulting series. In this way $\bar{\gamma}\approx 2\gamma$ was recovered. A similar procedure could be done in higher dimensions, but (since the physical interest is at larger g values) we found that this was not necessary; at higher dimensions G and $G-\chi$ exhibited similar behavior. Since additional operations degrade convergence, we did not make this the standard procedure in higher dimensions.

In the χ analysis here, we had to take derivative with respect to K twice to reconcile the K_c values obtained initially from the analysis of both series. (Such a small differ-

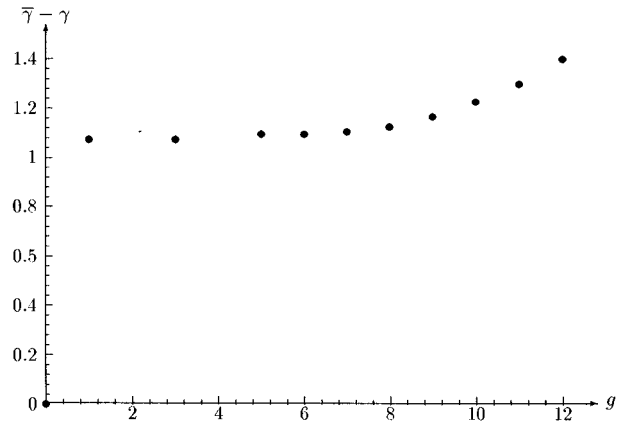

FIG. 7. Term-by-term divided series. Bimodal distribution. $d=5$.

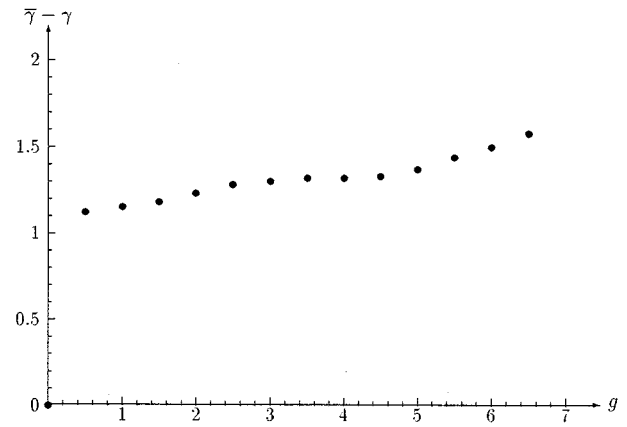

FIG. 9. Term-by-term divided series. Bimodal distribution. $d=4$.

TABLE IV. A selection of estimates of K_c, γ, and $\bar{\gamma}$ for $d=5$. Average $\bar{\gamma}-\gamma=1/2[(\bar{\gamma}-\gamma)_{M1}+(\bar{\gamma}-\gamma)_{M2}]$.

							Divided [a]		
		γ	γ	$\bar{\gamma}$	$\bar{\gamma}$	Average	$\bar{\gamma}-\gamma+1$		Average
g	$K=\beta J$	$M1$	$M2$	$M1$	$M2$	$\bar{\gamma}-\gamma$	$M1$	$M2$	$\bar{\gamma}-\gamma$
				Gaussian variable $d=5$					
8	$K_c=0.1315$	1.12	1.12	2.2	2.25	1.105	2.05	2.1	1.075
10	$K_c=0.136875$	1.13	1.135	2.25	2.25	1.1175	2.1	2.12	1.11
12	$K_c=0.142813$	1.14	1.14	2.32	2.32	1.18	2.16	2.16	1.16
14	$K_c=0.149298$	1.142	1.142	2.4	2.4	1.258	2.26	2.23	1.245
15	$K_c=0.152844$	1.144	1.144	2.45	2.45	1.306	2.3	2.28	1.29
18	$K_c=0.1665$	1.245	1.244						
20	$K_c=0.177$	1.28	1.28						
25	$K_c=0.213$	1.30	1.36						
				Bimodal variable $d=5$					
5	$K_c=0.125313$	1.0	1.08	2.15	2.1	1.085	2.07	2.12	1.095
7	$K_c=0.131375$	1.1	1.097	2.15	2.2	1.0765	2.08	2.12	1.1
8	$K_c=0.134918$	1.11	1.105	2.2	2.2	1.0925	2.1	2.12	1.11
9	$K_c=0.138875$	1.11	1.11	2.25	2.25	1.14	2.13	2.13	1.13
10	$K_c=0.1435$	1.135	1.135	2.3	2.35	1.19	2.2	2.2	1.2
11	$K_c=0.148813$	1.15	1.15						
12	$K_c=0.155248$	1.18	1.18						

[a]"Divided" refers to G/χ.

ence in the K_c values obtained from the independent analysis for the quantities which are known to be divergent at the same point usually comes from a big analytic additive term and can be eliminated by taking derivatives.) The results of the $M1$-$M2$ analysis in dimension three are given in Table VIII. The values of amplitude ratio A estimated at some of the g values are given in Table IX. The critical exponent γ is listed in Table II.

V. DISCUSSION AND CONCLUSIONS

Basically, our estimates for A were always close to unity. The fact that A was neither zero nor infinite, proves that $\bar{\gamma}=2\gamma$, i.e., that there exist only two independent exponents. The fact that A is close to one in all dimensions may seem like a confirmation of Eq. (13). Indeed, this was our preliminary conclusion in Ref. 54, based on some arguments from Ref. 22. However, although the deviations of A from unity are small, they are definitely nonzero, and they are larger for the bimodal distribution as compared to the Gaussian one. As discussed elsewhere,[53] these results for A agree with those obtained from a $1/d$ expansion for A in high dimensions. Thus, A is not universal, and the arguments of Ref. 22 clearly need revision at high dimensions. The theoretical situation at low d (viz. $d<d_>=6$) remains unclear.

Our results for the characterization of the second order transition are now quite complete. In three dimensions, we found good convergence at lower g values compared to where previous studies focused on. The crossover to this behavior from the usual Ising model at $g=0$ was very sharp indeed. The behavior for larger g values, where the exponents begin to increase with g, remains to be explained by future studies. The simplest explanation for this may be related to the fact that we derive the coefficients in our series as truncated power series in powers of g. These truncations may fail for large g. This increase may also simply arise due to the shortness of our series, and the large values of the coefficients for larger g. Another possibility is that there might be a crossover to tricritical behavior (as found in mean field theory). Series expansion methods do not handle tricritical points very easily when no low-temperature series are avaliable. A start on developing methods suited to the analysis of tricritical points has been made by Adler and Privman,[84] and some analysis using partial differential approximants will probably be required. Yet another possible explanation for the different behavior at large g may relate to the approach of the critical line to the zero temperature fixed point.[85]

TABLE V. Values of the amplitude ratio A [Eq. (13)] for selected choices of g at $d=5$.

			$d=5$				
			Values of Padé approximants for A				
g	Distribution	K_c	[7/6]	[6/7]	[6/6]	[5/6]	[6/5]
8	Gaussian	0.1315	1.01201	1.01201	1.01201	1.01200	1.01200
10	Gaussian	0.136875	1.01897	1.01897	1.01881	1.01836	1.01835
5	Bimodal	0.125313	1.10313	1.10313	1.10314	1.10313	1.10313
8	Bimodal	0.134918	1.18789	1.18807	1.17076	1.18681	1.18665

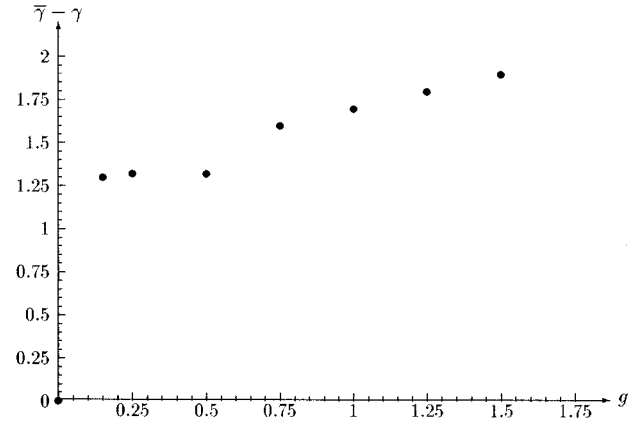

FIG. 10. Term-by-term divided series. Gaussian distribution. $d=3$.

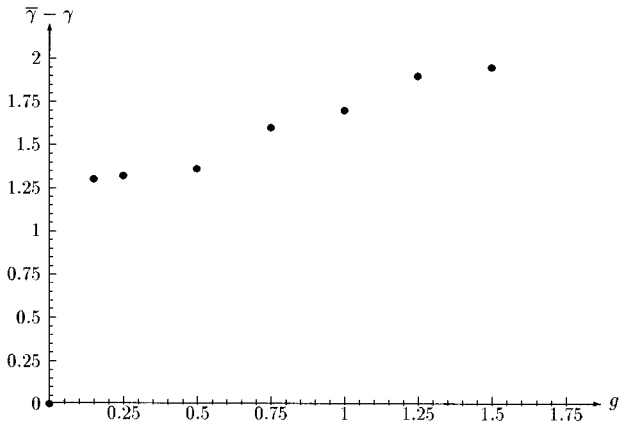

FIG. 11. Term-by-term divided series. Bimodal distribution. $d=3$.

In summary, our main achievements in this paper has been to derive 15 terms in the series for both G and χ for general dimension and g and for both Gaussian and bimodal field distributions, and to show that the critical behavior is determined by only two exponents. Our analysis of these series gave rather accurate values of the critical exponents γ and $\overline{\gamma}$, as summarized in Table III.

ACKNOWLEDGMENTS

We acknowledge discussions with J. Berger. This project has been supported by grants from the U. S.–Israel Binational Science Foundation (BSF) and the German–Israeli Foundation (GIF). A.B.H. also acknowledges partial support by the U.S.–Israel Educational Foundation and the National Science Foundation under Grant No. DMR-91-22784.

APPENDIX A: LIST OF THE CONTRIBUTING τ PRODUCTS FOR THE SUSCEPTIBILITY

$$t_1=\tau_i\tau_j, \tag{A1}$$

$$t_2=\tau_i^2\tau_j\tau_k,$$

$$t_3=\tau_i^2\tau_j^2,$$

$$t_4=\tau_i^2\tau_j^2\tau_k\tau_l,$$

$$t_5=\tau_i^3\tau_j^2\tau_k,$$

$$t_6=\tau_i^2\tau_j^2\tau_k^2,$$

$$t_7=\tau_i^3\tau_j^3,$$

$$t_8=\tau_i^2\tau_j^2\tau_k^2\tau_l\tau_m,$$

$$t_9=\tau_i^2\tau_j^2\tau_k^2\tau_l^2,$$

$$t_{10}=\tau_i^3\tau_j^2\tau_k^2\tau_l,$$

$$t_{11}=\tau_i^4\tau_j^2\tau_k^2,$$

$$t_{12}=\tau_i^4\tau_j^3\tau_k,$$

$$t_{13}=\tau_i^4\tau_j^4,$$

$$t_{14}=\tau_i^4\tau_j^2\tau_k\tau_l,$$

$$t_{15}=\tau_i^3\tau_j^3\tau_k^2,$$

$$t_{16}=\tau_i^2\tau_j^2\tau_k^2\tau_l^2\tau_m^2,$$

$$t_{17}=\tau_i^2\tau_j^2\tau_k^2\tau_l^2\tau_m\tau_n,$$

$$t_{18}=\tau_i^3\tau_j^3\tau_k^2\tau_l^2,$$

$$t_{19}=\tau_i^3\tau_j^2\tau_k^2\tau_l^2\tau_m,$$

$$t_{20}=\tau_i^4\tau_j^3\tau_k^2\tau_l,$$

$$t_{21}=\tau_i^4\tau_j^3\tau_k^3,$$

$$t_{22}=\tau_i^4\tau_j^2\tau_k^2\tau_l\tau_m,$$

$$t_{23}=\tau_i^4\tau_j^4\tau_k\tau_l,$$

$$t_{24}=\tau_i^4\tau_j^4\tau_k^2,$$

$$t_{25}=\tau_i^5\tau_j^4\tau_k,$$

$$t_{26}=\tau_i^5\tau_j^5,$$

$$t_{27}=\tau_i^5\tau_j^2\tau_k^2\tau_l,$$

$$t_{28}=\tau_i^5\tau_j^3\tau_k^2,$$

$$t_{29}=\tau_i^4\tau_j^2\tau_k^2\tau_l^2.$$

APPENDIX B: LIST OF THE CONTRIBUTING τ PRODUCTS FOR THE INTEGRATED CORRELATION FUNCTION

$$p_1=\tau_i^2\tau_j^2, \tag{B1}$$

$$p_2=\tau_i^2\tau_j^2\tau_k^2,$$

TABLE VI. A selection of estimates of K_c, γ, and $\bar{\gamma}$ for $d=4$. Average $\bar{\gamma}-\gamma=1/2[(\bar{\gamma}-\gamma)_{M1}+(\bar{\gamma}-\gamma)_{M2}]$.

g	$K=\beta J$	γ $M1$	γ $M2$	$\bar{\gamma}$ $M1$	$\bar{\gamma}$ $M2$	Average $\bar{\gamma}-\gamma$	Divided $\bar{\gamma}-\gamma+1$ $M1$	$M2$	Average $\bar{\gamma}-\gamma$
				Gaussian variable $d=4$					
3.5	$K=0.170625$	1.44	1.44	2.65	2.65	1.21	2.32	2.36	1.34
4	$K=0.1739$	1.39	1.39	2.68	2.72	1.31	2.35	2.4	1.35
5	$K=0.1815$	1.47	1.47	2.84	2.84	1.37	2.42	2.42	1.42
6	$K=0.1895$	1.45	1.45	2.9	2.9	1.45	2.44	2.44	1.44
7	$K=0.199$	1.52	1.52	3.05	3.05	1.53	2.52	2.54	1.53
				Bimodal variable $d=4$					
3	$K=0.1691$	1.38	1.38	2.62	2.65	1.255	2.3	2.4	1.35

TABLE VII. Values of the amplitude ratio A [Eq. (13)] for selected choices of g at $d=4$.

			$d=4$ Values of Padé approximants for A				
g	Distribution	K_c	[7/6]	[6/7]	[6/6]	[5/6]	[6/5]
3.5	Gaussian	0.170625	0.998679	0.998757	1.00605	1.04432	1.04229
6	Gaussian	0.1895	1.03960	1.03962	1.03750	1.03708	1.03708
3	Bimodal	0.1691	1.10827	1.10901	1.10721	1.10726	1.10726

TABLE VIII. A selection of estimates of K_c, γ, and $\bar{\gamma}$ for $d=3$. Average $\bar{\gamma}-\gamma=1/2[(\bar{\gamma}-\gamma)_{M1}+(\bar{\gamma}-\gamma)_{M2}]$.

g	$K=\beta J$	γ $M1$	γ $M2$	$\bar{\gamma}$ $M1$	$\bar{\gamma}$ $M2$	Average $\bar{\gamma}-\gamma$	Divided $\bar{\gamma}-\gamma+1$ $M1$	$M2$	Average $\bar{\gamma}-\gamma$
				Gaussian variable $d=3$					
0.15	$K=0.2268$	1.7		3.55		1.85	2.3		1.3
0.25	$K=0.2305$	2.1		3.7		1.6	2.32		1.32
0.50	$K=0.238$	2.1		3.85		1.75	2.32		1.32
0.75	$K=0.24675$	2.2		4.2		2.0	2.6		1.6
1.00	$K=0.25825$	2.7		4.85		2.15	2.7		1.7
				Bimodal variable $d=3$					
0.15	$K=0.2267$	1.75		3.55		1.8	2.3		1.3
0.25	$K=0.2304$	2.05		3.7		1.65	2.32		1.32
0.50	$K=0.238$	1.95		3.8		1.85	2.36		1.36
0.75	$K=0.2478$	2.25		4.25		2.0	2.6		1.6
1.00	$K=0.260$	2.75		4.85		2.1	2.75		1.75

TABLE IX. Values of the amplitude ratio A [Eq. (13)] for selected choices of g at $d=3$.

			$d=3$ Values of Padé approximants for A				
g	Distribution	K_c	[7/6]	[6/7]	[6/6]	[5/6]	[6/5]
0.15	Gaussian	0.2268	0.999905	0.999905	0.999929	0.999899	0.999899
0.75	Gaussian	0.24675	0.997862	0.997864	0.998095	0.997795	0.997791
0.15	Bimodal	0.2267	1.01017	1.00975	1.01011	1.01010	1.01010
0.75	Bimodal	0.2478	1.05644	1.06135	1.05260	1.05343	1.05334

$$p_3=\tau_i^2\tau_j^2\tau_k^2\tau_l^2, \qquad p_6=\tau_i^2\tau_j^2\tau_k^2\tau_l^2\tau_m^2,$$

$$p_4=\tau_i^4\tau_j^4, \qquad p_7=\tau_i^4\tau_j^2\tau_k^2\tau_l^2,$$

$$p_5=\tau_i^4\tau_j^2\tau_k^2, \qquad p_8=\tau_i^4\tau_j^4\tau_k^2.$$

APPENDIX C: SERIES EXPANSION OF THE SUSCEPTIBILITY OF THE RFIM IN GENERAL DIMENSION. GAUSSIAN DISTRIBUTION OF THE RANDOM FIELD

$$a(0)=1, \quad a(1)=2d, \quad a(2)=-2d+4d^2-g,$$

$$a(3)=4d/3-8d^2+8d^3-4dg,$$

$$a(4)=10d/3+16d^2/3-24d^3+16d^4+(4d-12d^2)g+2g^2,$$

$$a(5)=-116d/15+16d^2+24d^3-64d^4+32d^5+(-8d/3+24d^2-32d^3)g+10dg^2,$$

$$a(6)=-2224d/45+1748d^2/45+16d^3+272d^4/3-160d^5+64d^6+(-20d/3-20d^2+96d^3-80d^4)g+(-6d+36d^2)g^2-17g^3/3,$$

$$a(7)=42008d/315-1856d^2/5+3248d^3/15-64d^4/3+896d^5/3-384d^6+128d^7+(232d/15-40d^2-112d^3+320d^4-192d^5)g+(8d/3-56d^2+112d^3)g^2-92dg^3/3,$$

$$a(8)=108410d/63-848984d^2/315+3096d^3/5+1616d^4/5-224d^5+896d^6-896d^7+256d^8+(4448d/45-176d^2/5-80d^3-1504d^4/3+960d^5-448d^6)g+(-24d+80d^2-288d^3+320d^4)g^2+(-4d/3-120d^2)g^3+62g^4/3,$$

$$a(9)=-12453836d/2835+2828312d^2/189-2916680d^3/189+39200d^4/9+4928d^5/9-1024d^6+7552d^7/3-2048d^8+512d^9+(-84016d/315+13504d^2/15-6352d^3/15+128d^4/3-1920d^5+2688d^6-1024d^7)g+(100d/3-104d^2+464d^3-1152d^4+864d^5)g^2+(32d/9+96d^2-1216d^3/3)g^3+340dg^4/3,$$

$$a(10)=-1362578344d/14175+2767426988d^2/14175-35302448d^3/315+4622224d^4/945+22208d^5/3+6336d^6/5-11264d^7/3+20224d^8/3-4608d^9+1024d^{10}+(-216820d/63+98044d^2/21+2976d^3/5-1312d^4+1216d^5-6592d^6+7168d^7-2304d^8)g+(15136d/15-24316d^2/15+312d^3+6496d^4/3-4000d^5+2240d^6)g^2+(3080d/9-1304d^2/3+736d^3-3760d^4/3)g^3+(92d+456d^2)g^4-1382g^5/15,$$

$$a(11)=34816841408d/155925-4165970776d^2/4725+1843744832d^3/1575-578662816d^4/945+81720704d^5/945+63488d^6/5+60032d^7/15-12288d^8+17408d^9-10240d^{10}+2048d^{11}+(24907672d/2835-758008d^2/21+7215056d^3/189-60160d^4/9-10880d^5/3+7040d^6-62720d^7/3+18432d^8-5120d^9)g+(-580064d/315+31248d^2/5-103168d^3/15+704d^4+8896d^5-12672d^6+5632d^7)g^2+(-16984d/45+5224d^2/3-6848d^3/3+10816d^4/3-3648d^5)g^3+(-124d/9+208d^2/3+4792d^3/3)g^4-7448dg^5/15,$$

$$a(12)=725650999576d/93555-8606219416468d^2/467775+70193974864d^3/4725-59857682608d^4/14175-155226272d^5/945+141207488d^6/945+964352d^7/45+639488d^8/45-37376d^9+131072d^{10}/3-22528d^{11}+4096d^{12}+(2725156688d/14175-1729808848d^2/4725+9032704d^3/63+61005472d^4/945-76544d^5/3-168256d^6/15+90880d^7/3-62464d^8+46080d^9-11264d^{10})g+(-6282404d/105+799832d^2/7-292128d^3/5-2976d^4-2304d^5+33152d^6-37632d^7+13824d^8)g^2+(-1706528d/135+169808d^2/9-5648d^3/3-88832d^4/9+14400d^5-30464d^6/3)g^3+(-7874d/3+8648d^2/3-1320d^3+15440d^4/3)g^4+(-11992d/15-9948d^2/5)g^5+21844g^6/45,$$

$$a(13)=-101173799246512d/6081075+36124101224d^2/495-505539278768d^3/4455+32185348288d^4/405$$

$$-9929337632\,d^5/405+84744704\,d^6/45+34897408\,d^7/135+498176\,d^8/15+749056\,d^9/15-323584\,d^{10}/3$$
$$+321536\,d^{11}/3-49152\,d^{12}+8192\,d^{13}+(-69633682816\,d/155925+10036192528\,d^2/4725-2017736432\,d^3/675$$
$$+1350886592\,d^4/945-1954496\,d^5/63-346496\,d^6/5-599296\,d^7/15+112640\,d^8-178176\,d^9+112640\,d^{10}$$
$$-24576\,d^{11})g+(64694500\,d/567-11903968\,d^2/27+15047888\,d^3/27-778624\,d^4/3+42464\,d^5/3-26240\,d^6$$
$$+343040\,d^7/3-106496\,d^8+33280\,d^9)g^2+(16926304\,d/945-3633472\,d^2/45+3992224\,d^3/45-100928\,d^4/9$$
$$-119296\,d^5/3+50944\,d^6-81920\,d^7/3)g^3+(13372\,d/9-39344\,d^2/3+41048\,d^3/3-9792\,d^4+15648\,d^5)g^4$$
$$+(-8776\,d/45-11864\,d^2/5-105184\,d^3/15)g^5+22858\,dg^6/9,$$

$$a(14)=-36601976116480328\,d/42567525+96351271002572056\,d^2/42567525-7671835495928\,d^3/3465$$
$$+3368622438448\,d^4/3465-4089856928\,d^5/27-1908373568\,d^6/135+90820096\,d^7/27+84656128\,d^8/189$$
$$+37376\,d^9+501760\,d^{10}/3-299008\,d^{11}+258048\,d^{12}-106496\,d^{13}+16384\,d^{14}+(-1451301999152\,d/93555$$
$$+369215823568\,d^2/10395-116952256976\,d^3/4725+6293255824\,d^4/2835+319012352\,d^5/105-41765888\,d^6/135$$
$$-7246336\,d^7/45-2262784\,d^8/15+381952\,d^9-1469440\,d^{10}/3+270336\,d^{11}-53248\,d^{12})g+(884026688\,d/175$$
$$-53188140356\,d^2/4725+859424248\,d^3/105-1685537488\,d^4/945-862144\,d^5/3+226432\,d^6/3-143488\,d^7$$
$$+370688\,d^8-290304\,d^9+78848\,d^{10})g^2+(144898840\,d/189-154544248\,d^2/105+10641808\,d^3/15+216752\,d^4/3$$
$$-64192\,d^5/3-453632\,d^6/3+498176\,d^7/3-71424\,d^8)g^3+(1466248\,d/15-6926908\,d^2/45+54016\,d^3/3$$
$$+475792\,d^4/9-141280\,d^5/3+136640\,d^6/3)g^4+(159700\,d/9-62260\,d^2/3-10496\,d^3/5-68720\,d^4/3)g^5$$
$$+(30162\,d/5+49828\,d^2/5)g^6-929569\,g^7/315,$$

$$a(15)=1128557014030391416\,d/638512875-1763884756260386792\,d^2/212837625$$
$$+3040840729149634352\,d^3/212837625-265094921468288\,d^4/22275+113612045240512\,d^5/22275$$
$$-177949117568\,d^6/175+204767502592\,d^7/4725+1901840384\,d^8/315+27362304\,d^9/35-182272\,d^{10}/9$$
$$+23953408\,d^{11}/45-802816\,d^{12}+1835008\,d^{13}/3-229376\,d^{14}+32768\,d^{15}+(202347598493024\,d/6081075$$
$$-783024258928\,d^2/4455+1305217209808\,d^3/4455-16351895296\,d^4/81+757177792\,d^5/15+21175040\,d^6/9$$
$$-26821120\,d^7/27-4818944\,d^8/15-562176\,d^9+3639296\,d^{10}/3-1306624\,d^{11}+638976\,d^{12}-114688\,d^{13})g$$
$$+(-1475499215744\,d/155925+192390791648\,d^2/4725-284139209216\,d^3/4725+1335355744\,d^4/35$$
$$-981436352\,d^5/105-816256\,d^6/5+4457728\,d^7/15-618496\,d^8+1142784\,d^9-768000\,d^{10}+184320\,d^{11})g^2$$
$$+(-10095497464\,d/8505+1062358648\,d^2/189-4366996544\,d^3/567+95092768\,d^4/27-580928\,d^5/9$$
$$+76928\,d^6/3-4893184\,d^7/9+509952\,d^8-547840\,d^9/3)g^3+(-77875208\,d/945+2869792\,d^2/5$$
$$-32719648\,d^3/45+353824\,d^4/3+587584\,d^5/3-187776\,d^6+384256\,d^7/3)g^4+(91784\,d/225+247112\,d^2/3$$
$$-1392944\,d^3/15+52160\,d^4/3-355008\,d^5/5)g^5+(458776\,d/135+1000808\,d^2/45+1560464\,d^3/45)g^6$$
$$-4709644\,dg^7/315.$$

APPENDIX D: SERIES EXPANSION OF THE STRUCTURE FACTOR OF THE RFIM IN GENERAL DIMENSION. GAUSSIAN DISTRIBUTION OF THE RANDOM FIELD

$$a(0)=1,\quad a(1)=2\,d,\quad a(2)=-2\,d+4\,d^2,$$

$$a(3)=4\,d/3-8\,d^2+8\,d^3,\quad a(4)=10\,d/3+16\,d^2/3-24\,d^3+16\,d^4,$$

$$a(5)=-116\,d/15+16\,d^2+24\,d^3-64\,d^4+32\,d^5-2\,dg^2,$$

$$a(6)=-2224\,d/45+1748\,d^2/45+16\,d^3+272\,d^4/3-160\,d^5+64\,d^6+(6\,d-12\,d^2)g^2,$$

$$a(7)=42008\,d/315-1856\,d^2/5+3248\,d^3/15-64\,d^4/3+896\,d^5/3-384\,d^6+128\,d^7+(-16\,d/3+40\,d^2-48\,d^3)g^2+8\,dg^3,$$

$$a(8)=108410\,d/63-848984\,d^2/315+3096\,d^3/5+1616\,d^4/5-224\,d^5+896\,d^6-896\,d^7+256\,d^8+(-44\,d-8\,d^2+192\,d^3-160\,d^4)g^2+(-28\,d+56\,d^2)g^3,$$

$$a(9)=-12453836\,d/2835+2828312\,d^2/189-2916680\,d^3/189+39200\,d^4/9+4928\,d^5/9-1024\,d^6+7552\,d^7/3-2048\,d^8+512\,d^9+(1196\,d/15-248\,d^2-144\,d^3+768\,d^4-480\,d^5)g^2+(64\,d/3-192\,d^2+256\,d^3)g^3-92\,dg^4/3,$$

$$a(10)=-1362578344\,d/14175+2767426988\,d^2/14175-35302448\,d^3/315+4622224\,d^4/945+22208\,d^5/3+6336\,d^6/5-11264\,d^7/3+20224\,d^8/3-4608\,d^9+1024\,d^{10}+(6528\,d/5-7996\,d^2/5-72\,d^3-3104\,d^4/3+2720\,d^5-1344\,d^6)g^2+(872\,d/3-232\,d^2/3-1008\,d^3+960\,d^4)g^3+(116\,d-232\,d^2)g^4,$$

$$a(11)=34816841408\,d/155925-4165970776\,d^2/4725+1843744832\,d^3/1575-578662816\,d^4/945+81720704\,d^5/945+63488\,d^6/5+60032\,d^7/15-12288\,d^8+17408\,d^9-10240\,d^{10}+2048\,d^{11}+(-832112\,d/315+9424\,d^2-39136\,d^3/5+960\,d^4-5184\,d^5+8832\,d^6-3584\,d^7)g^2+(-6224\,d/15+1584\,d^2+384\,d^3-4480\,d^4+3200\,d^5)g^3+(-628\,d/9+2272\,d^2/3-1144\,d^3)g^4+128\,dg^5,$$

$$a(12)=725650999576\,d/93555-8606219416468\,d^2/467775+70193974864\,d^3/4725-59857682608\,d^4/14175-155226272\,d^5/945+141207488\,d^6/945+964352\,d^7/45+639488\,d^8/45-37376\,d^9+131072\,d^{10}/3-22528\,d^{11}+4096\,d^{12}+(-7366504\,d/105+13240832\,d^2/105-252448\,d^3/5-7968\,d^4+6336\,d^5-21504\,d^6+26880\,d^7-9216\,d^8)g^2+(-464096\,d/45+650272\,d^2/45-1216\,d^3+5184\,d^4-17600\,d^5+9856\,d^6)g^3+(-4478\,d/3+2776\,d^2/3+4120\,d^3-13840\,d^4/3)g^4+(-500\,d+1000\,d^2)g^5,$$

$$a(13)=-101173799246512\,d/6081075+36124101224\,d^2/495-505539278768\,d^3/4455+32185348288\,d^4/405-9929337632\,d^5/405+84744704\,d^6/45+34897408\,d^7/135+498176\,d^8/15+749056\,d^9/15-323584\,d^{10}/3+321536\,d^{11}/3-49152\,d^{12}+8192\,d^{13}+(398195516\,d/2835-107290336\,d^2/189+43382704\,d^3/63-262144\,d^4-18656\,d^5/3+31360\,d^6-237568\,d^7/3+77824\,d^8-23040\,d^9)g^2+(5344448\,d/315-345984\,d^2/5+1005376\,d^3/15-35968\,d^4/3+95744\,d^5/3-62976\,d^6+28672\,d^7)g^3+(73196\,d/45-22352\,d^2/3+424\,d^3+19648\,d^4-16480\,d^5)g^4+(736\,d/3-2912\,d^2+5120\,d^3)g^5-26914\,dg^6/45,$$

$$a(14)=-36601976116480328\,d/42567525+96351271002572056\,d^2/42567525-7671835495928\,d^3/3465+3368622438448\,d^4/3465-4089856928\,d^5/27-1908373568\,d^6/135+90820096\,d^7/27+84656128\,d^8/189+37376\,d^9+501760\,d^{10}/3-299008\,d^{11}+258048\,d^{12}-106496\,d^{13}+16384\,d^{14}+(26593877264\,d/4725-58032139468\,d^2/4725+2627465896\,d^3/315-1272505648\,d^4/945-1079296\,d^5/3-46336\,d^6/5+136064\,d^7-268288\,d^8+216576\,d^9-56320\,d^{10})g^2+(28546736\,d/45-54338896\,d^2/45+2874432\,d^3/5+35360\,d^4-57536\,d^5+150656\,d^6-209664\,d^7+79872\,d^8)g^3+(298408\,d/5-1400788\,d^2/15+19232\,d^3-165680\,d^4/9+250400\,d^5/3-54208\,d^6)g^4+(21568\,d/3-19664\,d^2/3-15648\,d^3+21504\,d^4)g^5+(35194\,d/15-70388\,d^2/15)g^6,$$

$$a(15)=1128557014030391416\,d/638512875-1763884756260386792\,d^2/212837625+3040840729149634352\,d^3/212837625-265094921468288\,d^4/22275+113612045240512\,d^5/22275-177949117568\,d^6/175+204767502592\,d^7/4725+1901840384\,d^8/315+27362304\,d^9/35-182272\,d^{10}/9+23953408\,d^{11}/45-802816\,d^{12}+1835008\,d^{13}/3-229376\,d^{14}+32768\,d^{15}+(-1684400264192\,d/155925+45522424432\,d^2/945-37204302784\,d^3/525+2676379040\,d^4/63-2699020096\,d^5/315-2390144\,d^6/5-1062656\,d^7/15+536576\,d^8-854016\,d^9+583680\,d^{10}-135168\,d^{11})g^2+(-3052769264\,d/2835$$

$$+300448432\,d^2/63-1185179200\,d^3/189+24702656\,d^4/9-675712\,d^5/9-260352\,d^6+1842176\,d^7/3-659456\,d^8$$
$$+215040\,d^9)g^3+(-74369096\,d/945+5444224\,d^2/15-6076064\,d^3/15+314336\,d^4/3-143808\,d^5+322432\,d^6$$
$$-503552\,d^7/3)g^4+(-94784\,d/15+31264\,d^2-10304\,d^3-78080\,d^4+80128\,d^5)g^5+(-156992\,d/135$$
$$+103048\,d^2/9-364592\,d^3/15)g^6+15736\,dg^7/5.$$

APPENDIX E: SERIES EXPANSION OF THE SUSCEPTIBILITY OF THE RFIM IN GENERAL DIMENSION. BIMODAL DISTRIBUTION OF THE RANDOM FIELD

$$a(0)=1,\quad a(1)=2\,d,\quad a(2)=-2\,d+4\,d^2-g,$$

$$a(3)=4\,d/3-8\,d^2+8\,d^3-4\,dg,$$

$$a(4)=10\,d/3+16\,d^2/3-24\,d^3+16\,d^4+(4\,d-12\,d^2)g+2\,g^2/3,$$

$$a(5)=-116\,d/15+16\,d^2+24\,d^3-64\,d^4+32\,d^5+(-8\,d/3+24\,d^2-32\,d^3)g+14\,dg^2/3,$$

$$a(6)=-2224\,d/45+1748\,d^2/45+16\,d^3+272\,d^4/3-160\,d^5+64\,d^6+(-20\,d/3-20\,d^2+96\,d^3-80\,d^4)g+(-2\,d/3$$
$$+20\,d^2)g^2-17\,g^3/45,$$

$$a(7)=42008\,d/315-1856\,d^2/5+3248\,d^3/15-64\,d^4/3+896\,d^5/3-384\,d^6+128\,d^7+(232\,d/15-40\,d^2-112\,d^3+320\,d^4$$
$$-192\,d^5)g+(-8\,d/9-24\,d^2+208\,d^3/3)g^2-188\,dg^3/45,$$

$$a(8)=108410\,d/63-848984\,d^2/315+3096\,d^3/5+1616\,d^4/5-224\,d^5+896\,d^6-896\,d^7+256\,d^8+(4448\,d/45-176\,d^2/5$$
$$-80\,d^3-1504\,d^4/3+960\,d^5-448\,d^6)g+(-296\,d/9+160\,d^2/3-160\,d^3+640\,d^4/3)g^2+(-232\,d/45$$
$$-368\,d^2/15)g^3+62\,g^4/315,$$

$$a(9)=-12453836\,d/2835+2828312\,d^2/189-2916680\,d^3/189+39200\,d^4/9+4928\,d^5/9-1024\,d^6+7552\,d^7/3-2048\,d^8$$
$$+512\,d^9+(-84016\,d/315+13504\,d^2/15-6352\,d^3/15+128\,d^4/3-1920\,d^5+2688\,d^6-1024\,d^7),g+(2428\,d/45$$
$$-472\,d^2/3+944\,d^3/3-2176\,d^4/3+608\,d^5)g^2+(1424\,d/135-64\,d^2/15-4864\,d^3/45)g^3+1004\,dg^4/315,$$

$$a(10)=-1362578344\,d/14175+2767426988\,d^2/14175-35302448\,d^3/315+4622224\,d^4/945+22208\,d^5/3+6336\,d^6/5$$
$$-11264\,d^7/3+20224\,d^8/3-4608\,d^9+1024\,d^{10}+(-216820\,d/63+98044\,d^2/21+2976\,d^3/5-1312\,d^4+1216\,d^5$$
$$-6592\,d^6+7168\,d^7-2304\,d^8)g+(154016\,d/135-1668\,d^2+616\,d^3/3+13472\,d^4/9-2720\,d^5+4928\,d^6/3)g^2$$
$$+(5020\,d/27-1568\,d^2/9+1744\,d^3/15-3632\,d^4/9)g^3+(3028\,d/315+520\,d^2/21)g^4-1382\,g^5/14175,$$

$$a(11)=34816841408\,d/155925-4165970776\,d^2/4725+1843744832\,d^3/1575-578662816\,d^4/945+81720704\,d^5/945$$
$$+63488\,d^6/5+60032\,d^7/15-12288\,d^8+17408\,d^9-10240\,d^{10}+2048\,d^{11}+(24907672\,d/2835-758008\,d^2/21$$
$$+7215056\,d^3/189-60160\,d^4/9-10880\,d^5/3+7040\,d^6-62720\,d^7/3+18432\,d^8-5120\,d^9)g+(-296608\,d/135$$
$$+335248\,d^2/45-334912\,d^3/45+6848\,d^4/9+6336\,d^5-9088\,d^6+12800\,d^7/3)g^2+(-194296\,d/675+10136\,d^2/9$$
$$-42944\,d^3/45+8384\,d^4/9-20288\,d^5/15)g^3+(-21428\,d/945+5216\,d^2/105+42808\,d^3/315)g^4-4424\,dg^5/2025,$$

$$a(12)=725650999576\,d/93555-8606219416468\,d^2/467775+70193974864\,d^3/4725-59857682608\,d^4/14175$$
$$-155226272\,d^5/945+141207488\,d^6/945+964352\,d^7/45+639488\,d^8/45-37376\,d^9+131072\,d^{10}/3-22528\,d^{11}$$
$$+4096\,d^{12}+(2725156688\,d/14175-1729808848\,d^2/4725+9032704\,d^3/63+61005472\,d^4/945-76544\,d^5/3$$
$$-168256\,d^6/15+90880\,d^7/3-62464\,d^8+46080\,d^9-11264\,d^{10})g+(-60878036\,d/945+7590664\,d^2/63$$
$$-57632\,d^3-14176\,d^4/3-2048\,d^5/3+73088\,d^6/3-84224\,d^7/3+10752\,d^8)g^2+(-16040384\,d/2025$$
$$+875336\,d^2/75-9056\,d^3/9-555968\,d^4/135+4736\,d^5-189056\,d^6/45)g^3+(-452486\,d/945+28136\,d^2/63$$

$$+1720\,d^3/21+38288\,d^4/63)g^4+(-159772\,d/14175-103028\,d^2/4725)g^5+21844\,g^6/467775,$$

$$\begin{aligned}a(13)=&-101173799246512\,d/6081075+36124101224\,d^2/495-505539278768\,d^3/4455+32185348288\,d^4/405\\&-9929337632\,d^5/405+84744704\,d^6/45+34897408\,d^7/135+498176\,d^8/15+749056\,d^9/15-323584\,d^{10}/3\\&+321536\,d^{11}/3-49152\,d^{12}+8192\,d^{13}+(-69633682816\,d/155925+10036192528\,d^2/4725-2017736432\,d^3/675\\&+1350886592\,d^4/945-1954496\,d^5/63-346496\,d^6/5-599296\,d^7/15+112640\,d^8-178176\,d^9+112640\,d^{10}\\&-24576\,d^{11})g+(1070048188\,d/8505-92423872\,d^2/189+344865872\,d^3/567-7248256\,d^4/27+83872\,d^5/9\\&-50560\,d^6/3+778240\,d^7/9-81920\,d^8+79360\,d^9/3)g^2+(184118848\,d/14175-38050432\,d^2/675\\&+40513696\,d^3/675-1087424\,d^4/135-16896\,d^5+293632\,d^6/15-555008\,d^7/45)g^3+(3279508\,d/4725\\&-1090192\,d^2/315+119432\,d^3/45-152896\,d^4/315+249248\,d^5/105)g^4+(1383464\,d/42525-145448\,d^2/1575\\&-2076064\,d^3/14175)g^5+648838\,dg^6/467775,\end{aligned}$$

$$\begin{aligned}a(14)=&-36601976116480328\,d/42567525+96351271002572056\,d^2/42567525-7671835495928\,d^3/3465\\&+3368622438448\,d^4/3465-4089856928\,d^5/27-1908373568\,d^6/135+90820096\,d^7/27+84656128\,d^8/189\\&+37376\,d^9+501760\,d^{10}/3-299008\,d^{11}+258048\,d^{12}-106496\,d^{13}+16384\,d^{14}+(-1451301999152\,d/93555\\&+369215823568\,d^2/10395-116952256976\,d^3/4725+6293255824\,d^4/2835+319012352\,d^5/105-41765888\,d^6/135\\&-7246336\,d^7/45-2262784\,d^8/15+381952\,d^9-1469440\,d^{10}/3+270336\,d^{11}-53248\,d^{12})g\\&+(225719111936\,d/42525-33296731292\,d^2/2835+7915472312\,d^3/945-4812590576\,d^4/2835-2892608\,d^5/9\\&+2723456\,d^6/45-927872\,d^7/9+862208\,d^8/3-228864\,d^9+191488\,d^{10}/3)g^2+(1481160748\,d/2835\\&-948937792\,d^2/945+11962288\,d^3/25+2463856\,d^4/45-1012288\,d^5/45-3012224\,d^6/45+3213056\,d^7/45\\&-173312\,d^8/5)g^3+(389940176\,d/14175-305236\,d^2/7+1720576\,d^3/315+10660112\,d^4/945-106784\,d^5/21\\&+378944\,d^6/45)g^4+(7282228\,d/8505-2396708\,d^2/2835-1846976\,d^3/4725-2198192\,d^4/2835)g^5\\&+(4960766\,d/467775+541172\,d^2/31185)g^6-929569\,g^7/42567525,\end{aligned}$$

$$\begin{aligned}a(15)=&1128557014030391416\,d/638512875-1763884756260386792\,d^2/212837625\\&+3040840729149634352\,d^3/212837625-265094921468288\,d^4/22275+113612045240512\,d^5/22275\\&-177949117568\,d^6/175+204767502592\,d^7/4725+1901840384\,d^8/315+27362304\,d^9/35-182272\,d^{10}/9\\&+23953408\,d^{11}/45-802816\,d^{12}+1835008\,d^{13}/3-229376\,d^{14}+32768\,d^{15}+(202347598493024\,d/6081075\\&-783024258928\,d^2/4455+1305217209808\,d^3/4455-16351895296\,d^4/81+757177792\,d^5/15+21175040\,d^6/9\\&-26821120\,d^7/27-4818944\,d^8/15-562176\,d^9+3639296\,d^{10}/3-1306624\,d^{11}+638976\,d^{12}-114688\,d^{13})g\\&+(-4705032378496\,d/467775+617317145056\,d^2/14175-908914247744\,d^3/14175+113567361632\,d^4/2835\\&-8872017088\,d^5/945-3834752\,d^6/15+2195200\,d^7/9-1404928\,d^8/3+905216\,d^9-1853440\,d^{10}/3\\&+151552\,d^{11})g^2+(-112565946616\,d/127575+11667913352\,d^2/2835-47600235008\,d^3/8505+204780128\,d^4/81\\&-793664\,d^5/27-251008\,d^6/9-6844928\,d^7/27+3586048\,d^8/15-846848\,d^9/9)g^3+(-3452242096\,d/99225\\&+955580368\,d^2/4725-1165450912\,d^3/4725+41096288\,d^4/945+1537472\,d^5/35-433024\,d^6/15\\&+1751296\,d^7/63)g^4+(-252009256\,d/212625+20746568\,d^2/2835-83177264\,d^3/14175-474176\,d^4/567\\&-16538048\,d^5/4725)g^5+(-52442296\,d/1403325+18472712\,d^2/155925+65701616\,d^3/467775)g^6\\&-35397196\,dg^7/42567525.\end{aligned}$$

APPENDIX F: SERIES EXPANSION OF THE STRUCTURE FACTOR OF THE RFIM IN GENERAL DIMENSION. BIMODAL DISTRIBUTION OF THE RANDOM FIELD

$$a(0)=1,$$

$$a(1)=2\,d,$$

$$a(2)=-2\,d+4\,d^2,$$

$$a(3)=4\,d/3-8\,d^2+8\,d^3,$$

$$a(4)=10\,d/3+16\,d^2/3-24\,d^3+16\,d^4,$$

$$a(5)=-116\,d/15+16\,d^2+24\,d^3-64\,d^4+32\,d^5-2\,dg^2,$$

$$a(6)=-2224\,d/45+1748\,d^2/45+16\,d^3+272\,d^4/3-160\,d^5+64\,d^6+(6\,d-12\,d^2)g^2,$$

$$a(7)=42008\,d/315-1856\,d^2/5+3248\,d^3/15-64\,d^4/3+896\,d^5/3-384\,d^6+128\,d^7+(-16\,d/3+40\,d^2-48\,d^3)g^2 +8\,dg^3/3,$$

$$a(8)=108410\,d/63-848984\,d^2/315+3096\,d^3/5+1616\,d^4/5-224\,d^5+896\,d^6-896\,d^7+256\,d^8+(-44\,d-8\,d^2+192\,d^3 -160\,d^4)g^2+(-12\,d+24\,d^2)g^3,$$

$$a(9)=-12453836\,d/2835+2828312\,d^2/189-2916680\,d^3/189+39200\,d^4/9+4928\,d^5/9-1024\,d^6+7552\,d^7/3-2048\,d^8 +512\,d^9+(1196\,d/15-248\,d^2-144\,d^3+768\,d^4-480\,d^5)g^2+(64\,d/9-256\,d^2/3+128\,d^3)g^3-12\,dg^4/5,$$

$$a(10)=-1362578344\,d/14175+2767426988\,d^2/14175-35302448\,d^3/315+4622224\,d^4/945+22208\,d^5/3+6336\,d^6/5 -11264\,d^7/3+20224\,d^8/3-4608\,d^9+1024\,d^{10}+(6528\,d/5-7996\,d^2/5-72\,d^3-3104\,d^4/3+2720\,d^5 -1344\,d^6)g^2+(520\,d/3-296\,d^2/3-496\,d^3+1600\,d^4/3)g^3+(76\,d/5-152\,d^2/5)g^4,$$

$$a(11)=34816841408\,d/155925-4165970776\,d^2/4725+1843744832\,d^3/1575-578662816\,d^4/945+81720704\,d^5/945 +63488\,d^6/5+60032\,d^7/15-12288\,d^8+17408\,d^9-10240\,d^{10}+2048\,d^{11}+(-832112\,d/315+9424\,d^2 -39136\,d^3/5+960\,d^4-5184\,d^5+8832\,d^6-3584\,d^7)g^2+(-9104\,d/45+2768\,d^2/3-2432\,d^4+1920\,d^5)g^3 +(-12\,d/5+112\,d^2-1048\,d^3/5)g^4+1696\,dg^5/945,$$

$$a(12)=725650999576\,d/93555-8606219416468\,d^2/467775+70193974864\,d^3/4725-59857682608\,d^4/14175 -155226272\,d^5/945+141207488\,d^6/945+964352\,d^7/45+639488\,d^8/45-37376\,d^9+131072\,d^{10}/3-22528\,d^{11} +4096\,d^{12}+(-7366504\,d/105+13240832\,d^2/105-252448\,d^3/5-7968\,d^4+6336\,d^5-21504\,d^6+26880\,d^7 -9216\,d^8)g^2+(-307424\,d/45+458368\,d^2/45-1408\,d^3+21824\,d^4/9-31040\,d^5/3+6272\,d^6)g^3+(-5942\,d/15 +6376\,d^2/15+3672\,d^3/5-1072\,d^4)g^4+(-4804\,d/315+9608\,d^2/315)g^5,$$

$$a(13)=-101173799246512\,d/6081075+36124101224\,d^2/495-505539278768\,d^3/4455+32185348288\,d^4/405 -9929337632\,d^5/405+84744704\,d^6/45+34897408\,d^7/135+498176\,d^8/15+749056\,d^9/15-323584\,d^{10}/3 +321536\,d^{11}/3-49152\,d^{12}+8192\,d^{13}+(398195516\,d/2835-107290336\,d^2/189+43382704\,d^3/63-262144\,d^4 -18656\,d^5/3+31360\,d^6-237568\,d^7/3+77824\,d^8-23040\,d^9)g^2+(9376448\,d/945-660992\,d^2/15+692288\,d^3/15 -28288\,d^4/3+54272\,d^5/3-39424\,d^6+57344\,d^7/3)g^3+(3892\,d/25-8848\,d^2/5+5096\,d^3/5+21568\,d^4/5 -4576\,d^5)g^4+(-16672\,d/2835-108512\,d^2/945+83456\,d^3/315)g^5-17014\,dg^6/14175,$$

$$a(14)=-36601976116480328\,d/42567525+96351271002572056\,d^2/42567525-7671835495928\,d^3/3465 +3368622438448\,d^4/3465-4089856928\,d^5/27-1908373568\,d^6/135+90820096\,d^7/27+84656128\,d^8/189$$

$$+37376\,d^9+501760\,d^{10}/3-299008\,d^{11}+258048\,d^{12}-106496\,d^{13}+16384\,d^{14}+(26593877264\,d/4725$$
$$-58032139468\,d^2/4725+2627465896\,d^3/315-1272505648\,d^4/945-1079296\,d^5/3-46336\,d^6/5+136064\,d^7$$
$$-268288\,d^8+216576\,d^9-56320\,d^{10})g^2+(9393008\,d/21-91481872\,d^2/105+6603712\,d^3/15+14112\,d^4$$
$$-40640\,d^5+93312\,d^6-137984\,d^7+55296\,d^8)g^3+(4670192\,d/225-8153644\,d^2/225+56288\,d^3/5-32464\,d^4/15$$
$$+21984\,d^5-86464\,d^6/5)g^4+(125936\,d/189-890672\,d^2/945-245792\,d^3/315+309376\,d^4/189/)g^5+(6926\,d/525$$
$$-13852\,d^2/525)g^6,$$

$$a(15)=1128557014030391416\,d/638512875-1763884756260386792\,d^2/212837625$$
$$+3040840729149634352\,d^3/212837625-265094921468288\,d^4/22275+113612045240512\,d^5/22275$$
$$-177949117568\,d^6/175+204767502592\,d^7/4725+1901840384\,d^8/315+27362304\,d^9/35-182272\,d^{10}/9$$
$$+23953408\,d^{11}/45-802816\,d^{12}+1835008\,d^{13}/3-229376\,d^{14}+32768\,d^{15}+(-1684400264192\,d/155925$$
$$+45522424432\,d^2/945-37204302784\,d^3/525+2676379040\,d^4/63-2699020096\,d^5/315-2390144\,d^6/5$$
$$-1062656\,d^7/15+536576\,d^8-854016\,d^9+583680\,d^{10}-135168\,d^{11})g^2+(-5972743664\,d/8505$$
$$+1845713200\,d^2/567-838117568\,d^3/189+18411200\,d^4/9-824960\,d^5/9-530176\,d^6/3+3625984\,d^7/9$$
$$-1355776\,d^8/3+153600\,d^9)g^3+(-8583584\,d/525+1641296\,d^2/15-3762336\,d^3/25+154336\,d^4/3$$
$$-535232\,d^5/15+492672\,d^6/5-299264\,d^7/5)g^4+(4701152\,d/14175+1998496\,d^2/945-64576\,d^3/21$$
$$-1673984\,d^4/315+516352\,d^5/63)g^5+(574528\,d/42525+285592\,d^2/2835-1334992\,d^3/4725)g^6$$
$$+7736\,dg^7/10395.$$

[1] S. Fishman and A. Aharony, J. Phys. C **12**, L729 (1979).
[2] J. F. Fernandez, Europhys. Lett. **5**, 129 (1988).
[3] P. G. de Gennes, J. Phys. Chem. **88**, 6469 (1984).
[4] S. B. Dierker and P. Wiltzius, Phys. Rev. Lett. **58**, 1865 (1987).
[5] M. Schwartz, J. Villain, Y. Shapir, and T. Natterman, Phys. Rev. B **48**, 3095 (1993).
[6] Y. Imry and S. K. Ma, Phys. Rev. Lett. **35**, 1399 (1975).
[7] G. Grinstein, Phys. Rev. Lett. **37**, 947 (1976).
[8] A. Aharony, Y. Imry, and S. K. Ma, Phys. Rev. Lett. **37**, 1364 (1976).
[9] A. P. Young, J. Phys. C **10**, L257 (1977).
[10] G. Parisi and N. Sourlas, Phys. Rev. Lett. **43**, 744 (1979).
[11] E. Lacour-Gayet and G. Toulouse, J. Phys. (Paris) **35**, 425 (1974).
[12] G. Grinstein and S. K. Ma, Phys. Rev. Lett. **49**, 685 (1982).
[13] J. Villain, J. Phys. (Paris) **43**, L551 (1982).
[14] K. Binder, Z. Phys. B **50**, 343 (1983).
[15] J. Z. Imbrie, Phys. Rev. Lett. **53**, 1747 (1984).
[16] J. Z. Imbrie, Commun. Math. Phys. **98**, 145 (1985).
[17] J. Bricmont and A. Kupiainen, Phys. Rev. Lett. **59**, 1829 (1987).
[18] J. Bricmont and A. Kupiainen, Commun. Math. Phys. **116**, 539 (1988).
[19] M. Schwartz and A. Soffer, Phys. Rev. Lett. **55**, 2499 (1985).
[20] M. Schwartz, Europhys. Lett. **15**, 777 (1991).
[21] M. Schwartz, J. Phys. C **18**, 135 (1985).
[22] M. Schwartz and A. Soffer, Phys. Rev. **33**, 2059 (1986).
[23] M. Schwartz, M. Gofman, and T. Nattermann, Physica A **178**, 6 (1991).
[24] A. J. Bray and A. J. MacKane, Europhys. Lett. **1**, 427 (1986).
[25] M. Mezard and A. P. Young, Europhys. Lett. **18**, 653 (1992).
[26] J. Villain, J. Phys. (Paris) **46**, 1843 (1985).
[27] A. J. Bray and M. A. Moore, J. Phys. C **18**, L927 (1985).
[28] D. S. Fisher, Phys. Rev. Lett. **56**, 4161 (1986).
[29] T. Nattermann, Phys. Status Solidi B **131**, 563 (1985).
[30] M. Schwartz, J. Phys. C **21**, 753 (1988).
[31] P.–z. Wong and J. W. Cable, Phys. Rev. B **28**, 5361 (1983).
[32] R. J. Birgeneau, Y. Shapira, G. Shirane, R. A. Cowley, and H. Yoshizawa, Physica B+C **135**, 83 (1986).
[33] D. P. Belanger, A. R. King, and V. Jaccarino, Phys. Rev. B **31**, 4538 (1985).
[34] J. Villain, Phys. Rev. Lett. **52**, 1543 (1984).
[35] R. Bruinsma and G. Aeppli, Phys. Rev. Lett. **52**, 1547 (1984).
[36] G. Grinstein and J. Fernandez, Phys. Rev. B **29**, 6389 (1984).
[37] Y. Kim and A. B. Harris, Phys. Rev. **32**, 4676 (1985).
[38] H. Yoshizawa and D. Belanger, Phys. Rev. B **30**, 5220 (1984).
[39] C. Ro, G. Grest, C. Soukoulis, and K. Levin, Phys. Rev. B **34**, 1681 (1985).
[40] U. Nowak and K. D. Usadel, Phys. Rev. B **44**, 7426 (1991).
[41] T. Natterman and P. Rujan, Int J. Mod. Phys. B **3**, 1597 (1989).
[42] T. Schneider and E. Pytte, Phys. Rev. B **15**, 1519 (1977).
[43] A. Aharony, Phys. Rev. B **18**, 3318 (1978).
[44] S. Galam and J. Birman, Phys. Rev. B **28**, 5322 (1983).
[45] R. Bruinsma, Phys. Rev. B **30**, 289 (1984).
[46] S. Galam and S. R. Salinas, J. Phys. C **18**, L439 (1985).

[47] A. P. Young and M. Nauenberg, Phys. Rev. Lett. **54**, 2429 (1985).
[48] A. T. Ogielski and D. A. Huse, Phys. Rev. Lett. **56**, 1298 (1986).
[49] A. Houghton, A. Khurana, and F. J. Seco, Phys. Rev. B **34**, 1700 (1986).
[50] H. Rieger and A. P. Young, J. Phys. A **26**, 5297 (1993).
[51] J. R. L. deAlmeida and R. Bruinsma, Phys. Rev. B **35**, 7267 (1987).
[52] In this paper what we refer to as the susceptibility, χ, is a dimensionless susceptibility $\chi = T\hat{\chi}$, where $\hat{\chi}$ is the usual susceptibility: $\sigma_i \sim \hat{\chi} h$.
[53] J. Berger, A. Aharony, J. Adler, and A. B. Harris (unpublished).
[54] M. Gofman, J. Adler, A. Aharony, A. B. Harris, and M. Schwartz, Phys. Rev. Lett. **71**, 1569 (1993); **71**, 2841(E) (1993).
[55] The ϵ expansion for $[\langle \vec{\phi}_{\mathbf{q}} \rangle_T \cdot \langle \vec{\phi}_{-\mathbf{q}} \rangle_T]|h$, using the methods of Refs. 8–10, yields that $\bar{\eta}(d)$ is equal to $\eta_0(d-2)$, where η_0 is the exponent for $g=0$. Also, one finds that $\eta(d) = \eta_0(d-2)$. Another derivation relies on $\theta = 2 - \bar{\eta} + \eta$ together with $\theta = 2$.
[56] T. Vojta and M. Schreiber, Phys. Rev. B **50**, 1272 (1994).
[57] Y. Shapir and A. Aharony, J. Phys. C **15**, 1361 (1982).
[58] A. Khurana, A. Houghton, and F. J. Seco, Phys. Rev. Lett. **54**, 357 (1985).
[59] A. Houghton, A. Khurana, and F. J. Seco, Phys. Rev. Lett. **55**, 856 (1985).
[60] A. T. Ogielski, Phys. Rev. Lett. **57**, 1251 (1986).
[61] After the appearance of Ref. 54, we received a preprint by H. Rieger, in which a discontinuity in the magnetization is obtained from Monte Carlo simulations. Following Ref. 54, he also found $\bar{\eta} = 2\eta$ and A close to unity.
[62] H. E. Cheung, Phys. Rev. B **33**, 6191 (1986).
[63] I. Dayan, M. Schwartz, and A. P. Young, J. Phys. A **26**, 3093 (1993).
[64] This tabulation is unpublished. It has been used in a number of other series calculations. See Ref. 83.
[65] A. B. Harris, Phys. Rev. B **26**, 337 (1982).
[66] A. B. Harris and Y. Meir, Phys. Rev. A **36**, 1840 (1987). See AIP document No. PAPS PLRAAN-36-1840-56 for 56 pages of weight list for all diagrams with no free ends having up to 15 bonds.
[67] A. B. Harris (unpublished). Here some mistakes in Eq. (8) of Ref. 65 are corrected. [A check on the correctness of Eq. (39) is that it gives zero when applied to diagrams with one or more free ends.]
[68] M. F. Sykes, D. S. Gaunt, P. D. Roberts, and J. A. Wyles, J. Phys. A **5**, 624 (1972).
[69] M. F. Sykes, D. S. Gaunt, P. D. Roberts, and J. A. Wyles, J. Phys. A **5**, 640 (1972).
[70] M. E. Fisher and D. S. Gaunt, Phys. Rev. **133**, A224 (1964).
[71] R. Fisch and A. B. Harris, Phys. Rev. B **41**, 11 305 (1990).
[72] M. Gofman, J. Adler, A. Aharony, A.B. Harris, and D. Stauffer, J. Stat. Phys. **71**, 1221 (1993).
[73] C. Munkel, D.W. Heermann, J. Adler, M. Gofman, and D. Stauffer, Physica A **193**, 540 (1993).
[74] F. J. Wegner, Phys. Rev. B **5**, 4529 (1972).
[75] J. Rudnick and D. R. Nelson, Phys. Rev. B **13**, 2208 (1976).
[76] J. L. Gammel, in *Padé Approximants and Their Applications*, edited by B. R. Graves-Morris (Academic Press, New York, 1973).
[77] J. Adler, M. Moshe, and V. Privman, *Percolation Structures and Processes*, edited by G. Deutscher, R. Zallen, and J. Adler (Adam Hilger, London, 1983), p. 337.
[78] J. Adler, I. Chang, and S. Shapira, J. Mod. Phys. C **4**, 1007 (1995).
[79] R. Roskies, Phys. Rev. B **24**, 5305 (1981).
[80] D. L. Hunter and G. A. Baker, Jr., Phys. Rev. B **7**, 3346 (1973).
[81] Y. Meir, J. Phys. A **20**, L349 (1987).
[82] J. Adler, A. Aharony, Y. Meir, and A. B. Harris, J. Phys. A **19**, 3631 (1986).
[83] J. Adler, Y. Meir, A. Aharony, A. B. Harris, and L. Klein, J. Stat. Phys. **58**, 511 (1990) and references therein.
[84] J. Adler and V. Privman, J. Phys. A **28**, 2445 (1995).
[85] R. Fisch (private communication).